Accepted Manuscript

Discovery and characterization of novel CYP1B1 inhibitors based on heterocyclic chalcones: Overcoming cisplatin resistance in CYP1B1-overexpressing lines

Neill J. Horley, Kenneth J.M. Beresford, Tarun Chawla, Glen J.P. McCann, Ketan C. Ruparelia, Linda Gatchie, Vinay R. Sonawane, Ibidapo S. Williams, Hoon L. Tan, Prashant Joshi, Sonali S. Bharate, Vikas Kumar, Sandip B. Bharate, Bhabatosh Chaudhuri

PII: S0223-5234(17)30081-8

DOI: 10.1016/j.ejmech.2017.02.016

Reference: EJMECH 9212

To appear in: *European Journal of Medicinal Chemistry*

Received Date: 16 December 2016

Revised Date: 6 February 2017

Accepted Date: 7 February 2017

Please cite this article as: N.J. Horley, K.J.M. Beresford, T. Chawla, G.J.P. McCann, K.C. Ruparelia, L. Gatchie, V.R. Sonawane, I.S. Williams, H.L. Tan, P. Joshi, S.S. Bharate, V. Kumar, S.B. Bharate, B. Chaudhuri, Discovery and characterization of novel CYP1B1 inhibitors based on heterocyclic chalcones: Overcoming cisplatin resistance in CYP1B1-overexpressing lines, *European Journal of Medicinal Chemistry* (2017), doi: 10.1016/j.ejmech.2017.02.016.

GRAPHICAL ABSTRACT

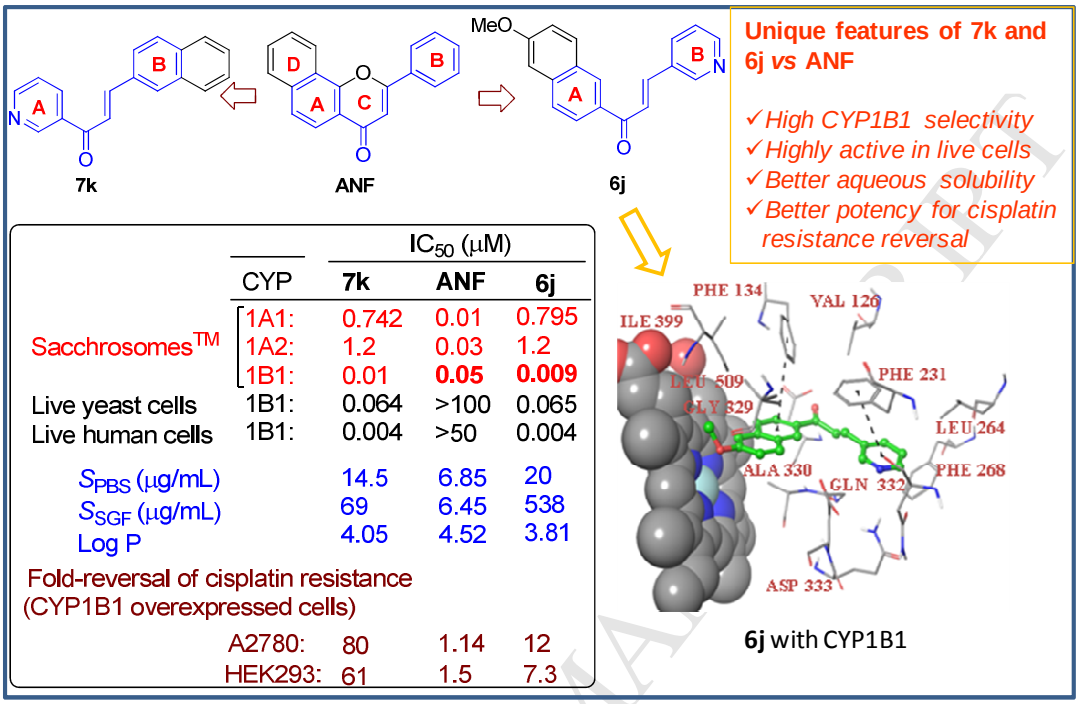

Pyridylchalcones were identified as potent and highly selective CYP1B1 inhibitors. These potent cell-permeable and water-soluble CYP1B1 inhibitors are likely to have useful roles in the treatment of cancer, glaucoma, ischemia and obesity.

Discovery and characterization of novel CYP1B1 inhibitors based on heterocyclic chalcones: Overcoming cisplatin resistance in CYP1B1-overexpressing lines

Neill J. Horley,[a,#] Kenneth J. M. Beresford,[a, #] Tarun Chawla,[a, #] Glen J. P. McCann,[a] Ketan C. Ruparelia,[a] Linda Gatchie,[b] Vinay R. Sonawane,[a] Ibidapo S. Williams,[b] Hoon L. Tan,[a] Prashant Joshi,[c] Sonali S. Bharate,[c] Vikas Kumar,[c] Sandip B. Bharate,[c,*] Bhabatosh Chaudhuri[a,b,*]

[a] School of Pharmacy, De Montfort University Leicester, LE1 7RH, UK.

[b] CYP Design Ltd, The Innovation Centre, 49 Oxford Street, Leicester, LE1 5XY, UK.

[c] Indian Institute of Integrative Medicine (CSIR), Canal Road, Jammu-180001, India.

[#] Contributed equally to the work described.

*Corresponding author

*Prof. Bhabatosh Chaudhuri, Professor of Cancer Studies,

Leicester School of Pharmacy, De Montfort University, Leicester, LE1 9BH, UK

Fax: Fax: +44(0) 116 257 7287; Tel: 44(0)116 250 7280

*E-mail: E-mail: bchaudhuri@dmu.ac.uk (BC),

*Dr. Sandip B. Bharate, Senior Scientist, Indian Institute of Integrative Medicine (CSIR), Canal Road, Jammu-180001, India. E-mail: sbharate@iiim.ac.in (SBB)

ABSTRACT

The structure of alpha-napthoflavone (ANF), a potent inhibitor of CYP1A1 and CYP1B1, mimics the structure of chalcones. Two potent CYP1B1 inhibitors **7k** (DMU2105) and **6j** (DMU2139) have been identified from two series of synthetic pyridylchalcones. They inhibit human CYP1B1 enzyme bound to yeast-derived microsomes (Sacchrosomes^{TM}) with IC_{50} values of 10 and 9 nM, respectively, and show a very high level of selectivity towards CYP1B1 with respect to the IC_{50} values obtained with CYP1A1, CYP1A2, CYP3A4, CYP2D6, CYP2C9 and CYP2C19 Sacchrosomes^{TM}. Both compounds also potently inhibit CYP1B1 expressed within 'live' recombinant yeast and human HEK293 kidney cells with IC_{50} values of 63, 65, and 4, 4 nM, respectively. Furthermore, the synthesized pyridylchalcones possess better solubility and lipophilicity values than ANF. Both compounds overcome cisplatin–resistance in HEK293 and A2780 cells which results from CYP1B1 overexpression. These potent cell-permeable and water-soluble CYP1B1 inhibitors are likely to have useful roles in the treatment of cancer, glaucoma, ischemia and obesity.

KEYWORDS:

Pyridylchalcones; cisplatin-resistance; CYP1B1 inhibitors; live CYP1B1-expressing human cells; live CYP1B1-expressing yeast cells; Sacchrosomes^{TM}

1. INTRODUCTION

The cytochrome P450 (CYP) enzyme superfamily plays a key role in the phase 1 oxidative metabolism and detoxification of both endogenous and xenobiotic substances [1]. However, certain members of the CYP superfamily of enzymes are also involved in the bio-activation of pro-carcinogens such as polyaromatic hydrocarbons, aromatic amines and nitro-polycyclic hydrocarbons [2-4]. The CYP1 subfamily of enzymes comprising 1A1, 1B1 and 1A2 fall into this category [5]. The CYP1A1 and CYP1B1 proteins are mainly expressed in extrahepatic tissues, while CYP1A2 is a major P450 found in the human liver (i.e. consisting of about 13% of the total CYP content in the human liver) [6]. CYP1B1 has been identified as a key enzyme in the carcinogenic action of 17-β-estradiol (E_2) and participates by catalysing hydroxylation at C-4 in E_2 to generate 4-hydroxyestradiol (4-OHE_2). Subsequent oxidation of 4-OHE_2 to estradiol-3,4-quinone results in a quinone-DNA adduct responsible for estrogen-related carcinogenesis. The other two members of the CYP1 family selectively metabolise E_2 to give 2-hydroxyestradiol which is not mutagenic [7].

CYP expression has been studied in a variety of human tumors. It is now recognized that many cancers have distinct P450 profiles and overexpress specific P450 protein sub-families. CYP1B1 is the only CYP1 family member that is significantly and consistently overexpressed in tumors [8-10]. CYP1B1 has been shown to be active within tumors and is also capable of metabolizing a structurally diverse range of anticancer drugs [11, 12]. Because of this, and its role in the activation of pro-carcinogens, CYP1B1 is seen as an important target for anticancer drug development. Selective inhibitors of this enzyme could have a major impact in cancer prevention. Particularly, as the extent of CYP1B1 expression appears to be a critical determinant of carcinogenesis in mammary, endometrial and ovarian tissues [7, 13-16].

It has been reported that CYP1B1 overexpression in normal mammalian cells leads to resistance to docetaxel [12], which is reversed in the presence of a CYP1B1 inhibitor [17]. Other chemotherapeutic agents which are subject to CYP1B1-mediated resistance include cisplatin, tamoxifen and nucleoside analogues [17-22]. Furthermore, it has been reported that CYP1B1 also plays a role in obesity. Disruption of the CYP1B1 gene in mice suppresses high-fat diet (HFD)-induced obesity suggesting that CYP1B1 is a potential target for identifying novel anti-obesity drugs [23]. Recently, it has been found that CYP1B1 contributes to the development of atherosclerosis and hypertension in apolipoprotein E-deficient mice which are known to rapidly develop severe hypercholesterolemia and spontaneous atherosclerotic lesions similar to those observed in humans. This would indicate that potent CYP1B1-specific inhibitors could be used for the treatment of atherosclerosis and hypertension caused by hypercholesterolemia [24, 25].

Human CYP1B1 shares only 38% amino acid sequence identity with CYP1A1 and 36% with 1A2 but seems to have an overlapping substrate profile with both, which makes the development of potent and selective inhibitors a significant challenge [26]. Despite this, a number of highly selective CYP1B1 inhibitors have been reported, several of these are based on the structure of resveratrol and its natural analogues. Notable examples include 2,4,2',6'-tetramethoxy-*trans*-stilbene (**1**) and 3,4,2'-trimethoxy-*trans*-stilbene (**2**) with IC_{50} values for CYP1B1 of 2 and 4 nM, respectively [26, 27]. Methoxyflavanoids have shown potent inhibition of CYP1B1, the naturally occurring flavone acacetin (**3**) having an IC_{50} value of 12 nM [28]. Methoxyflavones can also act as CYP1A1/CYP1B1 substrates, undergoing *O*-demethylation and aromatic hydroxylation reactions. It has been proposed that the metabolites of these reactions make a significant contribution to their anti-proliferative activities in cancer cells [29].

Alpha-naphthoflavone (ANF) (**4**) is a synthetic flavonoid and a strong CYP1 inhibitor [30]. Recently, it was used as a lead to design a series of trimethoxy-naphthoflavones of which compound **5** was the most potent and selective inhibitor of CYP1B1 (IC_{50} of 0.043 nM) [31]. A water-soluble naphthoflavone, in this series, also overcame the docetaxel-mediated drug resistance which was induced by the over-expression of CYP1B1 in MCF-7 breast cancer cells. Molecular modelling in this and other papers suggest that flavones bind into the active site of the CYP1 family enzymes with the B-ring orientated towards the heme prosthetic group. It seems that changing substituents on the B-ring has a profound effect on both activity and selectivity [28, 31].

Chalcones are precursors in the biosynthesis of flavones and are widely distributed in nature. They have received considerable attention due to their wide range of biological actions [32-39]; however, there are few reports of them acting as CYP1 inhibitors [30, 40]. Like methoxyflavones, certain chalcone derivatives are CYP1A1/CYP1B1 substrates, undergoing *O*-dealkylation and aromatic hydroxylation reactions. Comparing the chalcone and flavone structures, we reasoned that chalcones should fit into the narrow active site of CYP1B1 in a similar fashion to the flavones, with an aromatic ring adjacent to the heme iron [6]. If this ring was replaced by a group which could interact strongly with the heme iron, inhibition should result. Pyridine derivatives are known to inhibit CYP450 enzymes via coordination of the pyridine nitrogen to the heme iron and interactions of ring substituents with lipophilic regions of the enzyme pocket [41]. It has been reported that the addition of a suitably positioned pyridyl moiety to flavones improves their CYP450 inhibition by up to two orders of magnitude [41-43]. Herein, we report the synthesis and biological evaluation of a series of pyridylchalcones with the aim of finding potent and selective CYP1B1 inhibitors. Furthermore, it was conjectured that incorporating a pyridine ring into the flexible chalcone

structure would result in greater water solubility. Derivatives were prepared in which either the B or A-ring of the chalcone was replaced by a pyridyl group (shown in Figure 1A). The remaining ring was then altered in order to enhance inhibition and selectivity for CYP1B1. Molecular modeling was used to rationalize the empirical results obtained.

Figure 1

2. RESULTS AND DISCUSSION

2.1. Chemistry. The most common method for the synthesis of chalcones is the Claisen-Schmidt condensation reaction, in which equimolar quantities of a benzaldehyde and an acetophenone are reacted together with either a base or acid catalyst [44]. Typically, either sodium or potassium hydroxide is used with methanol as solvent. Initial attempts to prepare 3-(3-pyridyl)chalcones **6** using these standard conditions by reacting 3-pyridinecarboxaldehyde **9a** with an acetophenone **8a** were unsuccessful (Figure 1B). With 5 equivalents of aqueous sodium hydroxide at room temperature, little of the desired products were obtained. An alternative approach using aprotic anhydrous conditions (Figure 1B, Method 1) proved more fruitful. With 1 equivalent of freshly prepared lithium diisopropylamide (LDA) as base in THF, a series of pyridylchalones (Table 1) were prepared in yields of 25-88% after purification by flash chromatography. Reducing the amount of aqueous sodium hydroxide to 2 equivalents, and cooling the reaction to 0 °C for 2 h prior to warming to room temperature appeared to overcome initial difficulties. This method 2 was used to prepare further derivatives in yields of 8-61% (Table 1). For the synthesis of compound **6m**, 4-pyridinecarboxaldehyde (**9b**) was used in place of 3-pyridine carboxaldehyde (**9a**). Due to the poor solubility of the polyaromatic acetophenones in methanol during synthesis of **6n**, **6o** and **6p**, 25% of dichloromethane was added as a co-

solvent. An unexpected result was obtained in the reaction between **9a** and 3-chloroacetophenone **8** using method 2. Instead of the desired product **6g**, the major product of this reaction was the adduct **10**, presumably resulting from conjugate addition of the enolate of 3-chloroacetophenone to the previously formed chalcone **6g** (Figure 1B). A similar result was obtained with 3-bromoacetophenone. Although some chalcone was produced using the aprotic conditions (Method 1), it was not until a solvent free approach (Method 3) was adopted that these halogenated derivatives were prepared in acceptable yields [45]. No additional products were obtained under these conditions. 1-(3-Pyridyl)chalcones **7a-l** were prepared from the appropriate aldehydes **12** and 3-acetylpyridine **11** using either methods 2 or 3. Yields ranged from 13-76% after purification by flash chromatography (Table 2).

2.2. Yeast microsomes (Sacchrosomes^{TM}) as a screening tool for CYP1 inhibitors. The human *CYP1B1* gene was isolated from a human liver cDNA library that was constructed by BioCat (Germany). The baker's yeast, *Saccharomyces cerevisiae*, was chosen for the production of human CYPs because the intracellular architecture of the compartments within yeast cells closely resembles that of human cells. Because of this, yeast cells have been widely used as a model to study human biochemical pathways and to express heterologous human proteins [46-48]. The details of CYP1B1 expression in baker's yeast are provided in supporting information (Section S2). The presence of the CYP1B1 protein in the CYP1B1 Sacchrosomes was confirmed using Western blotting. The activity of the CYP1B1-Sacchrosomes (microsomal membranes isolated from recombinant yeast cells) was then compared with that of CYP1B1-Supersomes^{TM} (microsomal membranes isolated from recombinant insect cells and obtained from Corning-Gentest). The Supersomes, isolated from insect cells, are recognised as the benchmark for commercially produced recombinant CYP450s across the world. Results indicated that relative CYP1B1 activity in Sacchrosomes

is around 3-fold higher than that present in Supersomes (Section S3 of supporting information). It can be argued that the much higher activity of CYP1B1 seen in Sacchrosomes, when compared to the insect cell derived CYP1B1-Supersomes, could be due to the intracellular organization of yeast being akin to that of human cells and that this may have influenced the increased activity of the CYP1B1-Sacchrosomes. Hence, it became clear that the yeast-derived human microsomal CYP1B1 enzyme could, in theory, be used for rapid screening of the potential CYP1B1 inhibitors **6-7** that had been synthesized.

Before embarking on screening the pyridylchalcone structure-based library of compounds, it was essential that one proved that the active site of the CYP1B1-Sacchrosomes was similar in conformation to the reported recombinant CYP1B1 enzymes. Therefore, the ability of ANF, a known inhibitor of CYP1B1, to inhibit CYP1B1-Sacchrosomes was investigated. ANF is not a specific inhibitor for any of the CYP1 family of enzymes [31]. It inhibits all the CYP1 enzymes (CYP1A1, CYP1A2 and CYP1B1) to a certain degree. Results with CYP1B1-Sacchrosomes showed that there was >80% inhibition at 1 µM of ANF. Its IC_{50} for inhibition of yeast-produced CYP1B1 enzyme was found to be 0.008 µM (Section S4 of supporting information) which was close to the published value of 0.005 µM for ANF observed using CYP1B1 enzyme isolated from a recombinant human lymphoblastoid cell line [49]. ANF's IC_{50} for inhibition of CYP1A1-Sacchrosomes is 0.01 µM and of CYP1A2-Sacchrosomes is 0.03 µM, which are close to published values obtained with CYP1A1-Supersomes and CYP1A2-Supersomes, 0.018 µM and 0.012 µM, respectively [50, 51]. This re-affirmed the validity of using CYP-bearing Sacchrosomes for further CYP inhibition studies.

2.3. Screening of pyridylchalcones for CYP1 inhibition in yeast microsomes (Sacchrosomes^{TM}). After confirming the validity of Sacchrosomes, containing active CYP1B1 enzyme, they were used for screening of the pyridylchalcones **6a-p** and **7a-l**. The

compounds were first tested at a single concentration of 5 µM to test their effects on CYP1B1 activity. A percentage inhibition value for each of the compounds in the library was obtained after testing each compound twice. The compounds with the best percentage inhibition were chosen for determination (in triplicate) of IC_{50}s, in at least three separate experiments; the values are presented in Tables 1 and 2.

Table 1 and 2

The graphs obtained for **7k** and **6j** in CYP1B1-bearing Sacchrosomes using 7-ethoxyresorufin (7-ER) (5 µM final concentration) as substrate, are depicted in Section S10 of the supporting information. The results indicate that **7k** and **6j** are indeed potent inhibitors of CYP1B1 showing IC_{50} values of 10 and 9 nM, respectively. Amongst all the compounds screened, the compounds bearing a naphthyl ring were found to be the most potent. Among naphthyl linked compounds those with a pyridin-3-yl on the other side were better CYP1B1 inhibitors than **6m** which has a pyridine-4-yl ring.

2.4. Specificity of the potent CYP1B1 inhibitors 7k and 6j in Sacchrosomes. Since ANF is a non-specific inhibitor of the CYP1 family of enzymes [6, 51, 52], it was important to determine if the compounds identified as CYP1B1 inhibitors in the CYP1B1-Sacchrosome screen, were specific to CYP1B1 (Tables 1 and 2). Hence, Sacchrosomes™ containing CYP1A1 and CYP1A2 were used to test the ability of the two compounds to inhibit these CYP1 enzymes. It was found that the two most potent inhibitors identified, **7k** and **6j**, were specific. Compound **7k** shows 74 and 120-fold selectivity for CYP1B1 over CYP1A1 and CYP1A2, whereas **6j** shows 88 and 133-fold selectivity over the same enzymes.

Later, the most potent CYP1B1 inhibitors (i.e. IC_{50} < 0.1 µM) which showed specificity towards CYP1B1 were selected and tested for the inhibition of CYP2D6 and CYP3A4

Sacchrosomes. The CYP2D6 and CYP3A4 enzymes are involved in the metabolism of the majority of approved pharmaceuticals. If any of the chalcone based CYP1B1-specific inhibitors are to be developed for further therapeutic use, it is essential that they do not inhibit these two enzymes. Medicinal entities which inhibit CYP2D6 or CYP3A4 have the potential of being involved in drug-drug interactions in patients who are prescribed more than one drug. The results obtained are presented in Tables 1 and 2. They indicate that, for the CYPs investigated, the two most potent inhibitors of CYP1B1, **7k** and **6j**, are CYP1B1-specific.

2.5. Pyridylchalcones 7k and 6j potently inhibit CYP1B1 expressed within live yeast cells. The two most potent CYP1B1-specific inhibitors were tested in live yeast cells to establish if the compounds could penetrate the cell wall of live eukaryotic cells. We chose recombinant CYP1B1-bearing baker's yeast *S. cerevisiae* cells for our studies, this yeast being a unicellular eukaryote. The majority of this particular yeast's proteins share a high degree of homology with the primary sequences of human proteins. It was conjectured that, if the compounds did penetrate yeast cells to inhibit CYP1B1 bound to the endoplasmic reticular membranes, they could find therapeutic applications in human cells (which are multicellular eukaryotes) that overexpress CYP1B1 under certain diseased conditions.

The graphs that allowed the determination of the IC_{50}s of **7k** and **6j**, in live yeast cells using 7-ER (with 5 μM final concentration) as substrate, are depicted in Section S11 of the supporting information. These compounds showed IC_{50} values of 64 and 65 nM, respectively. The results indicate that the two most potent chalcone-based CYP1B1 inhibitors can enter live yeast cells to inhibit the endoplasmic reticular membrane-bound CYP1B1. This would suggest that **7k** and **7j** could further be assessed for their possible therapeutic potential in human cells. The two IC_{50} values in recombinant yeast cells are almost identical, as was seen in the assay using CYP1B1 Sacchrosomes. The IC_{50} value for a compound is always

expected to be higher in cellular assays since all chemical compounds have some affinity towards both extracellular and intracellular membranes. Hence, one can conclude that there is a correlation between the results obtained from the yeast live cell assays and those obtained with microsomal CYP1B1 enzyme borne on Sacchrosomes. This highlights the fact that the CYP1B1-bearing live yeast cells, developed here for these studies, could provide an inexpensive route towards the screening of potential inhibitors of CYP1B1 which could have roles in the treatment of cancer, glaucoma, ischemia and obesity.

2.6. Pyridylchalcones 7k and 6j potently inhibit CYP1B1 enzyme expressed within live human cells. In the pharmaceutical industry, CYP450 assays are often performed in hepatocytes grown in suspension, where studies normally cannot last for more than 6 hours because of the rapid degradation of CYP enzyme activities. Hepatocytes contain a conglomeration of CYPs and it is often difficult, if not impossible, to precisely determine IC_{50} values of an inhibitor of a specific CYP of interest using convenient fluorescence-based assay protocols which depend on the inhibition of specific CYP-mediated conversion of a non-fluorescent substrate to a fluorescent product. This is also true when using CYP-specific chemical substrates, with medicinal properties, for IC_{50} determinations of potential CYP inhibitors.

Until now, CYP assays have never been attempted in live recombinant human 'suspension' cells that over-express specific human *CYP* genes. We have adapted adherent human kidney HEK293 cells for growth in suspension. These cells were transfected with an expression plasmid (pCDM/hCYP1B1; pCDM obtained from CYP Design) encoding the same human *CYP1B1* gene which had been cloned previously in a yeast expression plasmid (details are provided in section S5 of supporting information). The graphs that allowed determination of the IC_{50}s of **7k** and **6j**, in live human HEK293 cells, are depicted in section S12 of the

supporting information. At each concentration of the compound, cells were incubated for 30 min. Two different substrates, 7-ER and 3-cyano-7-ethoxycoumarin (CEC) were used for determining the inhibitory capacity of the two compounds. IC_{50} values were found to be in the range of 4-53 nM, for both compounds. As mentioned before, 7-ER is converted to fluorescent resorufin by CYP1B1 enzyme activity, whereas the same enzyme converts CEC to 3-cyano-7-hydroxycoumarin. In both biotransformation reactions, CYP1B1 is responsible for de-ethylation.

The results indicate that two compounds potently inhibit the human CYP1B1 enzyme that resides on the endoplasmic reticular membranes within human cells. It can be conceived that the enzyme activity within human HEK293 cells would be closely mimicking the activities in human tissues which overexpress CYP1B1 protein under certain diseased conditions like cancer and obesity. Although the tissues involved in these diseases are different, the proteins present in the endoplasmic reticular membranes, to which CYP1B1 must be bound to manifest activity, should be the same (if not identical) in all tissue types. Thus the newly developed assay, based on HEK293 cells grown in suspension, can open up new avenues for rapid screening of potential CYP1B1 inhibitors which would be directly pertinent to further pre-clinical studies. In fact, we have shown that 200-300 compounds can be screened without automation, per week, in such CYP-expressing human cell assays (manuscript in preparation). The extraordinary CYP1B1-inhibiting potency of **7k** and **6j**, corroborated in live human cells, did open up the possibility of further exploring the compounds' therapeutic potential in the context of human diseases like cancer.

2.7. Pyridylchalcones 7k and 6j overcome cisplatin resistance in adherent HEK293 cells that overexpress CYP1B1. pcDNA3.1/hCYP1B1 (Figure S7, in section S6, of supporting information), is a plasmid where the *hCYP1B1* gene was cloned in the vector pcDNA3.1

(Invitrogen) with the view of creating stable adherent cell lines. CYP1B1 protein expression was confirmed through Western blotting (Figure 2A). Mechanically scraped cells, after transfection, showed CYP1B1 enzyme activity (albeit far lower than in the same number of suspension cells) using 7-ER as substrate (results not shown).

Figure 2

We also observed that overexpression of CYP1B1 protein, from the pcDNA3.1/hCYP1B1 (Figure 2A), in adherent HEK293 cells results in resistance to cisplatin when compared to cells that do not express CYP1B1. Resistance was observed by determining EC_{50} values (i.e. the concentration of cisplatin that provides half-maximal response to cell growth) by monitoring cell viability in the presence of cisplatin (Figure 2B). We then attempted to find out if the two potent CYP1B1-specific inhibitors, **7k**, **6j**, can overcome resistance to cisplatin observed in CYP1B1 overexpressing HEK293 cells. The results show that the two CYP1B1-specific inhibitors can indeed overcome CYP1B1-mediated resistance to cisplatin (Figure 2C). Figure 2C shows that upon co-administration of CYP1B1-specific inhibitors with cisplatin in HEK293 cells, transfected with pcDNA3.1/hCYP1B1, the cisplatin resistant cells become re-sensitized to cisplatin. EC_{50} values of cisplatin in the presence of **7k** and **6j** abruptly diminish from the EC_{50} value seen using cells which were not treated with CYP1B1 inhibitors. In the presence of **6j**, the EC_{50} is reversed back to 8.3 µM from 61 µM (seen in CYP1B1-expressing cells without any inhibitor). The EC_{50} value, in the presence of **6j**, resembles the EC_{50} of cisplatin, 8.7 µM, in cells transfected with the empty plasmid which has no *CYP1B1* gene and therefore cannot express CYP1B1 protein.

In the presence of **7k** however, the EC_{50} goes down to 1 µM indicating that the cells had suffered from toxicity which may have been mediated by CYP1B1 inhibition. Un-transfected cells (HEK293: pcDNA3.1), when treated with cisplatin and **7k** (10 x IC_{50}) did not show any

perceptible decrease of cisplatin EC_{50} (8.5 µM ± 0.9). ANF, the known inhibitor of CYP1 enzymes reduces the cisplatin EC_{50} from 61 µM (seen in the presence of CYP1B1 overexpression from the pcDNA3.1 plasmid) only to 40 µM. This is much higher than 8.7 µM (seen with the cell line transfected with the control plasmid) indicating that ANF may not be effective in reversing resistance to cisplatin.

2.8. Sensitization of CYP1B1-overproducing ovarian cancer cells, resistant to cisplatin, by treatment with pyridyl chalcones 7k and 6j. Gene expression studies comparing cisplatin-sensitive and cisplatin-resistant ovarian cancer cells, A2780 and A2780cis, have shown, using real time RT-PCR (reverse transcriptase mediated PCR), that *CYP1B1* is a gene, amongst five genes, that is highly elevated in resistant A2780cis cells compared to sensitive A2780 cells (section S6 of supporting information) [53]. We show that indeed CYP1B1 protein is selectively overproduced in the cisplatin-resistant A2780cis cells when compared with the parent A2780 cells (Figure 3A). Western blotting confirms the earlier proteomic studies [53].

Figure 3

In analogy to results obtained with HEK293 cells (Figure 2B), the ovarian cancer cell line A2780 when transfected with the plasmid pcDNA3.1/CYP1B1 (Figure 3A) also showed resistance to cisplatin. Resistant cells could be sensitised once again by the two CYP1B1-specific inhibitors, **7k** and **6j** (Figure 3B).

Although we could measure CYP1B1 activity in mechanically scraped A2780cis cells, unfortunately we have not been able to show that the resistant cells can be re-sensitised to cisplatin using the two potent CYP1B1-specific inhibitors. The supplier of the cell line (ECACC) states that the cisplatin-resistant A2780cis cells (catalogue no. 93112517),

developed by chronic exposure of the parent cisplatin-sensitive A2780 cell line (ECACC catalogue no. 93112519) to increasing concentrations of cisplatin, has an increased ability to repair DNA damage as well as has cytogenetic abnormalities. We have wondered whether these were the reasons for our observations with our potent CYP1B1 inhibitors.

2.9. Experimental solubility and lipophilicity of ANF (4) and pyridylchalcones 6j and 7k. ANF has been reported as highly insoluble in water because of its rigid and polyaromatic (hydrophobic) structure. Furthermore, it has been reported that it precipitates in cell culture medium at 5 µM concentration [31]. It is well reported fact that the incorporation of structural flexibility in planar and rigid structures results in improved aqueous solubility. The pyridylchalcones prepared herein, were expected to possess better solubility and lipophilicity than ANF, because of its increased flexibility than ANF. In order to find out the comparative solubility and lipophilicity profile of ANF and pyridyl chalcones, we determined their experimental solubility (in three biological media *viz*. PBS, SGF and SIF) and lipophilicity. Results are presented in Table 3. ANF showed poor solubility in all three media with solubility values less than 6.85 µg/ml. The predicted Log P/ Log D values were also very high (4.52 and 4.87, respectively). Pyridylchalcones showed 2-3 fold improvement in solubility in PBS. However, highly significant improvement (83-fold increase) in the solubility of **6j** in simulated gastric fluid (SGF: pH 1.2) was observed. The improvement in solubility was corroborated in lipophilicity values, as both pyridylchalcones have improved Log P/ Log D values when compared to ANF.

Table 3

2.10. Molecular modelling studies of pyridylchalcones 7k and 6j with a panel of CYP enzymes. ANF is a well-known pan-inhibitor of CYP1 family isoforms with poor selectivity (<10-fold difference in selectivity for 1B1 over 1A1). Interactions of ANF with CYP1

isoforms 1A1, 1B1 and 1A2 has been reported in co-crystallized structures [6, 51, 52]. Molecular modelling studies indicate that, unlike ANF, the hydrophobic 6-methoxynaphthyl group (ring A and D) of chalcone **6j** co-ordinates with the heme molecule (distance is <5 Aº) and interacts with hydrophobic residue Phe134. It leads to an alignment of the flexible semi-polar linker with the peptide bond between Ala330-Gly329 in I helix. Further, the π electron cloud of the heteroaromatic pyridyl ring (ring B) interacts with the conserved Phe231 residue of the distorted F helix to complete the slot-like structure as shown in Figure 4b. However, in the case of **7k**, the flexible linker between the two hydrophobic rings (A and B) is in the reverse position with the heteroatom present in ring A. This leads to the exposure of bulkier hydrophobic naphthyl group to the deeper catalytic pocket where it interacts with the heme molecule (distance is <5 Aº). The reverse linker also has close alignment with the peptide bond of Ala330-Gly329 in I helix at one side of the slot cavity. The π electron cloud of the heteroaromatic pyridyl ring (ring B) interacts with the conserved Phe231 residue of the distorted F helix and the conserved Phe134 residue of B-C loop by π-π interactions (Figure 4c).

The 180 ºC flip in orientation of the A and B rings of **6j** with respect to the chromene nucleus of ANF towards the heme molecule is due to the compact size of the binding cavity where a phenyl or 6-methoxynaphthyl ring can easily be accommodated while a benzo(h)chromene nucleus is not. The driving force for the binding of **6j** seems to be the additional hydrophobic interactions of the A ring with the hydrophobic Phe123 residue of the binding cavity. However, in the case of **7k** the semi-polar linker is present in a reverse orientation, and the size of the naphthyl ring is smaller than the benzo(h)chromene nucleus which allows it to fit in the binding cavity, thereby enabling the naphthyl group (ring B) to coordinate with the heme molecule.

Both **6j** and **7k** are specific to the CYP1B1 enzyme isoform within the CYP1 family. They inhibit the CYP1B1 isoform with >74 fold selectivity in comparison with the 1A1 and 1A2 isoforms, which could possibly be due to the differences in amino acid residues in the primary sequences of these enzymes (only 38% and 36% sequence homology of CYP1A1 and CYP1A2, with CYP1B1). To gain a deeper understanding of the experimentally observed selectivity, the binding sites of CYP1B1, CYP1A1 and CYP1A2 were aligned with respect to both compounds. It was observed that, in the case of **6j**, the 6-methoxynaphthyl group (ring A) interacts with Phe134 residue by additional hydrophobic π-π interactions. This crucial interaction was not present in the 1A1 and 1A2 isoforms, due to the 180 ºC flip in orientation of **6j** (see section S9 of supporting information) in the active site of enzyme. However, in the case of **7k** a difference exists in the interacting amino acid residues despite having a similar interaction pattern. The structural difference in the CYP1 family members and their interactions with the inhibitors **6j** and **7k** rationalize the manifold difference in selectivity, as shown in Figure 4d.

CYP2 and CYP3 family members CYP3A4, CYP2D6, CYP2C9 and CYP2C19 are involved in the metabolism of most pharmaceuticals and consequently their inhibition is the major reason for drug-drug interactions. The lower tendency to inhibit CYP2 and CYP3 family members and specificity towards CYP1 family enzymes indicate that both **7k** and **6j** would be free from any possible drug-drug interactions. The observed trend in selectivity toward CYP1B1 enzyme over CYP3A4, CYP2D6 could be due to the lack of interactions of both **7k** and **6j** with the heme iron (distance is >5.0 Aº). Moreover, in CYP1B1 enzyme, I helix is aligned to the semipolar linker of **6j** and **7k** and aromatic naphthyl and pyridyl rings were stabilized by π electron cloud of multiple phenyl alanine residues. These non-bonded interactions are missing in CYP2D6 and CYP3A4 enzymes. The literature [54-57] on

CYP3A4 inhibitors indicates that the presence of pyridyl or imidazolyl ring in the inhibitor drastically improves potency due to heme ligation by the heteroaromatic *N* atom. However, our observations indicate that such heteroatom-heme ligation does not appear to be the crucial factor for higher potency against CYP1 family enzymes. This could be due to the binding site of CYP1 family enzymes being compact in nature in contrast to the CYP2 and CYP3 family enzymes which comprise large and flexible binding sites to accommodate a wide range of xenobiotics. Based on these observations, it may be concluded that heme chelation is not a crucial factor for CYP1 family enzyme inhibition by pyridylchalcones.

Figure 4

3. CONCLUSIONS

Based on a pyridylchalcone structure, a small library of compounds was synthesized with a view to identifying CYP1B1 inhibitors. A number of promising molecules were detected, with several being CYP1B1-specific. Two of the most potent molecules, **7k** and **6j**, were further evaluated for their inhibitory potential in live yeast and human cell assays. In order to do this, novel cellular assays were devised. After confirmation of their potencies and CYP1B1-specificity, the compounds were evaluated to determine if they could overcome cisplatin resistance mediated by CYP1B1 overproduction, having already established that CYP1B1 is one of five proteins which is overproduced in cisplatin-resistant cells. It was seen that the cisplatin resistance mediated by CY1B1 overproduction could be overcome in both HEK293 cells and an ovarian cancer cell line, A2780. The identified pyridylchalcones possess better water solubility and lower lipophilicity than ANF, which makes them show better effect in cell based assays.

These results open up avenues for further pre-clinical evaluation of the anticancer potential of **7k** and **6j** in SCID mice-human tumour models. Because of the compounds' CYP1B1

inhibitory potencies and remarkable specificities they may also find applications in animal models for ischemia, obesity and glaucoma.

4. EXPERIMENTAL SECTION

4.1. General. All solvents and chemicals were used as purchased without further purification. The ^{1}H and ^{13}C-NMR spectra were recorded on a Bruker Avance AV400 NMR spectrometer at 30°C. Chemical shifts are reported in δ units (ppm) relative to either TMS or the residual solvent signal. IR spectra were recorded as KBr discs on a Perkin-Elmer 298 spectrophotometer. HRMS was performed using a Thermo Scientific LTQ Orbitrap XL at the EPSRC National Mass Spectrometry Service Centre (Swansea, UK). Melting points (uncorrected) were determined on a Gallenkamp melting point apparatus in open glass capillary tubes. TLC was performed on Merck Silica Gel $60f_{254}$ coated plates. Plates were visualised under UV light (254/366nm) and stained with either 2,4-dinitrophenylhydrazine, iodine or phosphomolybdic acid. Fluka Silica gel 60 (30-45μ) was used for flash chromatography. The purities of compounds were determined using either elemental analyses (C, H, N) or HPLC. The former was performed on a CE440 elemental analyser by Warwick Analytical Services. Results were within ±0.4% of the theoretical values. HPLC was carried out on a Perkin Elmer 200 series chromatography system using a HAISIL 100 C18 (250 x 4.6mm) column eluting with 60 % acetonitrile/ water (Flow rate = 1.0 mL/ min, λ = 300 nm.). All samples had purity greater than 95%.

4.2. General methods for chalcone synthesis

Method 1: A solution of n-butyl lithium (3.13 mL, 1.6 M in hexanes, 5.0 mmol) was added dropwise to a stirred solution of *N*,*N*-diispropylethylamine (0.87 mL, 5.0 mmol) in anhydrous THF (10 mL) at -78°C under nitrogen. After 30 min a solution of the acetophenone (5.0 mmol) in anhydrous THF (5 mL) was added followed, after 10 min, by a solution of the

aldehyde (5.0 mmol) in THF (5 ml). The reaction was allowed to warm to RT and stirred overnight. After quenching with water (20 mL) the resulting mixture was neutralized with 1M hydrochloric acid and extracted with ethyl acetate (3x50 mL). The combined organics extracts were washed with brine (20 ml), dried ($MgSO_4$) and the solvent removed under vacuum. Products were purified by flash chromatography on silica using a gradient elution with hexane: ethyl acetate: triethylamine (10 to 80% ethyl acetate, 5% triethylamine).

Method 2: Aqueous sodium hydroxide solution (50% w/v, 0.8 mL, 10 mmol) was added to a stirred solution of the aectophenone (5.0 mmol) and aldehyde (5.0 mmol) in methanol (20 mL) at 0°C. The resulting mixture was stirred at 0°C for two hours before warming up to rt overnight. The reaction was quenched with water (20 mL), neutralised with 1M hydrochloric acid and extracted with ethyl acetate (3x50 mL). The combined organic layers were washed with saturated brine (20 mL), dried ($MgSO_4$) and the solvent removed under vacuum. Products were purified as in method 1.

Method 3: The aectophenone (6.4mmol) and aldehyde (6.4 mmol) were mixed and then ground with powdered sodium hydroxide (0.26 g, 6.4mmol) using a pestle and mortar. This was continued until no further change in consistency and colour was observed. The resulting mixture was dissolved in a mixture of ethyl acetate and water (200 mL, 3: 1). The organic layer was partitioned, washed with saturated brine (20 mL), dried ($MgSO_4$) and the solvent removed under vacuum. Products were purified as in method 1.

4.2.1. (E)-1-(3-Methoxyphenyl)-3-(3-pyridinyl) prop-2-en-1-one (6a, DMU713): Method 1; Light brown solid (25%). mp 83-84°C; ^{1}H NMR ($CDCl_3$): δ 3.90 (3H, s), 7.15 (1H, dd, *J* = 3.7, 8.8 Hz), 7.36 (1H, dd, *J* = 4.7, 8.8 Hz), 7.43 (1H, t, *J* = 8.4 Hz), 7.54-7.63 (3H, m), 7.79 (1H, d, *J* = 15.8 Hz), 7.93-7.98 (1H, m), 8.64 (1H, dd, *J* = 1.9, 4.7 Hz), 8.87 (1H, d, *J* = 2.7

Hz). ^{13}C NMR ($CDCl_3$): δ 55.48, 112.90, 119.61, 120.77, 121.30,123.84, 129.69, 130.65, 139.08, 140.90, 150.3, 151.11, 159.96, 189.49; IR (KBr) /cm^{-1} 1663 (C=O); HRMS found [M+1]+ 240.1019, $C_{15}H_{13}NO_2$ requires [M+1]+ 240.1019; Anal. Calcd $C_{15}H_{13}NO_2$: C, 75.30; H, 5.48, N, 5.85; Found C, 75.53; H, 5.42; N, 5.67.

4.2.2. (E)-1-(4-Methoxyphenyl)-3-(3-pyridinyl)prop-2-en-1-one (6b, DMU714)*[44, 58]* Method 1; Yellow solid (48%). mp 105-106°C; ^{1}H NMR ($CDCl_3$): δ 3.90 (3H, s), 7.00 (2H, d, *J* = 8.8 Hz), 7.35 (1H, dd, *J* = 4.6, 8.3 Hz), 7.61 (1H, d, *J* = 16.2 Hz), 7.78 (1H, d, *J* = 16.2 Hz), 7.92-7.96 (1H, m), 8.04 (2H, d, *J* = 8.8 Hz), 8.62 (1H, dd, *J* = 4.2, 1.3 Hz), 8.87 (1H, d, *J* = 2.5 Hz); ^{13}C NMR ($CDCl_3$): δ55.55, 114.00, 123.77, 130.69, 130.90, 134.56, 137.38, 140.08, 149.88, 150.93, 163.72, 188.02; IR (KBr) /cm^{-1} 1662 (C=O); HRMS found [M+1]+ 240.1017, $C_{15}H_{13}NO_2$ requires [M+1]+ 240.1019; Anal. Calcd $C_{15}H_{13}NO_2.0.15H_2O$: C, 74.46; H, 5.54, N, 5.79; Found C, 74.41; H, 5.43; N, 5.77.

4.2.3. (E)-1-(2, 4-Dimethoxyphenyl)-3-(3-pyridinyl) prop-2-en-1-one (6c, DMU715)*[44, 58]* Method 1; Bright yellow solid (55%). mp 91-93°C; ^{1}H NMR ($CDCl_3$): δ 3.88 (3H, s), 3.92 (3H, s), 6.52 (1H, d, *J* = 2.3 Hz), 6.58 (1H, dd, *J* = 2.3, 9.4 Hz), 7.34 (1H, dd, *J* = 5.3, 7.0 Hz), 7.58-7.94 (2H, m), 7.81 (2H, d, *J* = 9.4 Hz), 7.86-7.94 (1H, m), 8.59 (1H, dd, *J* = 1.2, 5.4 Hz), 8.84 (1H, d, *J* = 2.4 Hz); ^{13}C NMR ($CDCl_3$): δ55.60, 55.78, 98.65, 105.46, 121.75, 123.69, 129.07, 131.35, 133.17, 134.64, 137.81, 149.73, 150.51, 160.65, 164.60, 189.59; IR (KBr) /cm^{-1} 1656 (C=O); HRMS found [M+1]+ 270.1126, $C_{16}H_{15}NO_3$ requires [M+1]+ 270.1125; Anal. Calcd $C_{16}H_{15}NO_3$: C, 71.36; H, 5.61, N 5.20 Found C, 71.03; H, 5.65 N 5.18.

4.2.4. (E)-1-(3, 4-Dimethoxyphenyl)-3-(3-pyridyl) prop-2-en-l-one (6d, DMU716). Method 1; Light yellow solid (37%). mp 91-93°C; ^{1}H NMR ($CDCl_3$): δ 3.99 (6H, s), 6.94

(1H, d, *J* = 7.5 Hz), 7.36 (1H, dd, *J* = 5.0, 8.0 Hz), 7.63 (1H, d, *J* = 15.9 Hz), 7.64 (1H, d, *J* = 2.0 Hz), 7.68 (1H, dd, *J* = 2.0, 7.5 Hz), 7.78 (1H, d, *J* = 15.9 Hz), 7.93-7.96 (1H, m), 8.63 (1H, dd, *J* = 1.5, 5.0 Hz), 8.87 (1H, d, *J* = 1.5 Hz); ^{13}C NMR ($CDCl_3$) δ 56.18, 109.96, 110.81, 122.70, 123.69, 124.50, 130.91, 134.59, 140.10, 149.40, 149.87, 150.86, 153.69, 187.94; IR (KBr) /cm^{-1} 1655 (C=O); HRMS found [M+1]+ 270.1125, $C_{16}H_{15}NO_3$ requires [M+1]+ 270.1125; Anal. Calcd $C_{16}H_{15}NO_3$: C, 71.36; H, 5.61, N, 5.20; Found C, 71.03; H, 5.65; N, 5.14.

4.2.5. (E)-1-(3, 5-Dimethoxyphenyl)-3-(3-pyridyl) prop-2-en-l-one (6e, DMU717) Method 1: Yellow solid (34%). mp 90-91°C; ^{1}H NMR ($CDCl_3$): δ 3.87 (6H, s), 7.69 (1H, t, *J* = 2.1 Hz), 7.15 (2H, d, *J* = 2.1 Hz), 7.37 (1H, dd, *J* = 4.8, 6.4 Hz), 7.54 (1H, d, *J* = 16.0 Hz), 7.78 (1H, d, *J* = 16.0 Hz), 7.92-7.96 (1H, m), 8.63 (1H, dd, *J* = 1.6, 4.8 Hz), 8.86 (1H, d, *J* = 1.6 Hz); ^{13}C NMR ($CDCl_3$): δ 55.67, 105.30, 106.45, 123.78, 123.92, 130.67, 134.54, 139.73, 141.02, 150.06, 151.16, 161.03, 189.47; IR (KBr) /cm^{-1} 1666 (C=O); HRMS found [M+1]+ 270.1124, $C_{16}H_{15}NO_3$ requires [M+1]+ 270.1125; Purity >99 % HPLC (Retention time 12.012 min).

4.2.6. (E)-3-(3-Pyridyl)-1-(2, 3, 4-trimethoxyphenyl)prop-2-en-l-one (6f, DMU718)[58, 59]Synthetic Method 1; Yellow solid (51%). mp 77-78°C; ^{1}H NMR ($CDCl_3$): δ 3.92 (3H, s) 3.93 (3H, s), 3.94 (3H, s), 6.67 (1H, d, *J* = 8.8 Hz), 7.34 (1H, dd, *J* = 5.2, 7.2 Hz), 7.53 (1H, d, *J* = 8.8 Hz), 7.59 (1H, d, *J* = 16.0 Hz), 7.68 (1H, d, *J* = 16.0 Hz), 7.70-7.94 (1H, m), 8.61 (1H, dd, *J* = 1.0, 5.2 Hz), 8.83 (1H, d, *J* = 2.1 Hz); ^{13}C NMR ($CDCl_3$): δ56.17, 61.07, 62.09, 107.50, 123.74, 126.04, 126.27, 128.46, 131.05, 134.47, 138.73, 142.18, 149.95, 150.77, 153.97, 157.48, 189.98; IR (KBr) /cm^{-1} 1666 (C=O); HRMS found [M+1]+ 300.1229, $C_{17}H_{17}NO_4$ requires [M+1]+ 300.1230; Purity >99 % % HPLC (Retention time 12.168 min).

4.2.7. (E)-1-(3-Chlorophenyl)-3-(3-pyridinyl)prop-2-en-1-one (6g, DMU2123) Method 3; Pale yellow solid (52%). mp 128-130^{o}C; ^{1}H NMR ($CDCl_3$): δ 7.37 (1H, dd, *J* = 5.2, 7.7 Hz), 7.45 (1H, t, *J* = 6.6 Hz), 7.51-7.60 (2H, *m*), 7.80 (1H, d, *J* = 16.0 Hz), 7.89 (1H, d, *J* = 7.6 Hz), 7.94-8.02 (2H, m), 8.65 (1H, d, *J* = 5.2 Hz), 8.86 (1H, s); ^{13}C NMR ($CDCl_3$): δ 123.19, 123.84, 126.60, 128.62, 130.09, 130.40, 133.04, 135.07, 139.30, 141.77, 150.15, 151.40, 188.44; IR (KBr) /cm^{-1} 1665 (C=O); HRMS found [M+1]+ 244.0524, $C_{14}H_{10}NOCl$ requires [M+1]+ 244.0524; Anal. Calcd $C_{14}H_{10}NOCl$: C, 69.00; H, 4.14, N, 5.75; Found C, 68.86; H, 4.12, N, 5.66.

4.2.8. (E)-1-(3-Bromophenyl)-3-(3-pyridinyl)prop-2-en-1-one (6h, DMU2127) Method 3; Pale yellow solid (39%). mp 126-128^{o}C; ^{1}H NMR (DMSO-d_6): δ 7.51 (1H, dd, *J* = 7.4, 3.9 Hz), 7.56 (1H, t, *J* = 7.7 Hz), 7.81 (1H, d, *J* = 15.8 Hz), 7.87-7.92 (1H, m), 8.11 (1H, d, *J* = 15.8 Hz), 8.16-8.19 (1H, m), 8.35-8.42 (2H, m), 8.64 (1H, dd, *J* = 2.1, 7.4 Hz), 9.06 (1H, d, *J* = 2.8 Hz); ^{13}C NMR (DMSO-d_6) δ122.36, 123.41, 123.88, 127.58, 130.37, 131.04, 135.31, 135.96, 139.27, 141.36, 150.54, 151.17, 187.65; IR (KBr) /cm^{-1} 1665 (C=O); HRMS found [M]+ 288.0025, $C_{14}H_{10}BrNO$ requires [M]+ 288.0019; Anal. Calcd $C_{14}H_{10}BrNO$: C, 58.36; H, 3.50, N, 4.86; Found C, 58.26; H, 3.44; N, 4.83.

4.2.9. (E)-1-(2-Naphthyl)-3-(3-pyridyl)prop-2-en-1-one (6i, DMU745) Method 1; Pale brown solid (52%). mp 117-118°C; ^{1}H NMR ($CDCl_3$): δ 7.38 (1H, dd, *J* = 4.2, 7.8 Hz), 7.55-7.63 (2H, m), 7.75 (1H, d, *J* = 16.0 Hz), 7.86 (1H, d, *J* = 16.0 Hz), 7.90 (1H, d, *J* = 8.6 Hz), 7.96 (1H, d, *J* = 9.3 Hz), 7.98-8.02 (2H, m), 8.10 (1H, dd, *J* = 2.6, 9.3 Hz), 8.53 (1H, s), 8.64 (1H, dd, *J* = 1.9, 4.2 Hz), 8.90 (1H, d, *J* = 2.6 Hz); ^{13}C NMR ($CDCl_3$) δ 123.80, 123.89, 124.37, 126.94, 127.88, 128.76, 128.76, 129.58, 130.15, 130.77, 132.56, 134.65, 135.12, 135.64, 140.86, 150.05, 151.14, 189.58; IR (KBr) /cm^{-1} 1651 (C=O); HRMS found [M]+

260.1072, $C_{18}H_{13}NO$ requires [M]+ 260.1070; Purity >99 % HPLC (Retention time 11.757 min).

4.2.10. (E)-1-(6-Methoxy-2-naphthyl)-3-(3-pyridyl)prop-2-en-1-one (6j, DMU2139) Method 2: Pale yellow solid (8%). mp 133-134°C; ^{1}H NMR ($CDCl_3$): δ 3.96 (3H, s), 7.18 (1H, d, *J* = 2.9 Hz), 7.23 (1H, dd, *J* = 3.3, 8.8 Hz), 7.28 (1H, dd, *J* = 7.3, 4.4 Hz), 7.75 (1H, d, *J* = 15.0 Hz), 7.80-7.92 (3H, m), 7.97-8.02 (1H, m), 8.09 (1H, dd, *J* = 8.4, 2.2 Hz), 8.48 (1H, s), 8.64 (1H, dd, *J* = 4.3, 2.2 Hz), 8.90 (1H, d, *J* = 2.6 Hz); ^{13}C NMR ($CDCl_3$): δ 55.47, 105.89, 119.88, 123.78, 123.89, 125.12, 127.45, 127.88, 130.09, 130.89, 131.18, 133.14, 134.62, 137.40, 140.42, 149.99, 151.03, 159.96, 189.13; IR (KBr) /cm^{-1} 1643 (C=O); HRMS found [M]+ 290.1175, $C_{19}H_{15}NO_2$ requires [M]+ 290.1176; Purity >99 % HPLC (Retention time 15.732 min).

4.2.11. (E)-1-(1-Naphthyl)-3-(3-pyridyl)prop-2-en-1-one (6k, DMU746) Method 1; Brown solid (88%). mp 123-124°C; ^{1}H NMR ($CDCl_3$): δ 7.34 (1H, dd, *J* = 8.2, 4.6 Hz), 7.38 (1H, d, *J* = 16.0 Hz), 7.52-7.64 (4H, m), 7.80 (1H, dd, *J* = 7.3, 1.0 Hz), 7.88-7.94 (2H, m), 8.02 (1H, d, *J* = 4.3 Hz), 8.36 (1H, dd, *J* = 8.2, 1.4 Hz), 8.62 (1H, dd, *J* = 1.3, 4.1 Hz), 8.78 (1H, d, *J* = 1.3 Hz); ^{13}C NMR ($CDCl_3$): δ 123.83, 124.50, 125.56, 126.63, 127.47, 128.55, 128.74, 130.48, 132.12, 134.53, 136.49, 150.07, 151.24, 194.76; IR (KBr) /cm^{-1} 1662 (C=O); HRMS found [M]+ 260.1070, $C_{18}H_{13}NO$ requires [M]+ 260.1070; Purity 99 % HPLC (Retention time 10.333 min).

4.2.12. (E)-1-(4-Biphenyl)-3-(3-pyridyl)prop-2-en-1-one (6l, DMU2134) Method 2; Yellow solid (27%). m p 140-141°C; ^{1}H NMR (DMSO-d_6): δ 7.40-7.56 (4H, m), 7.76-7.83 (3H, m), 7.89 (2H, d, *J* = 9.2 Hz), 8.14 (1H, d, *J* = 14.6 Hz), 8.27 (2H, d, *J* = 9.2 Hz), 8.36-8.40 (1H, m), 8.62 (1H, dd, *J* = 1.0, 4.4 Hz), 9.04 (1H, d, *J* = 1.9 Hz); ^{13}C NMR (DMSO-d_6)

δ188.40, 151.01, 150.37, 144.72, 140.52, 138.82, 136.06, 135.17, 130.51, 128.46, 123.95, 123.86. IR (KBr) /cm^{-1} 1659 (C=O); HRMS found [M]+ 286.1224, $C_{20}H_{16}ON$ requires [M]+ 286.1226; Purity 96 % HPLC (Retention time 14.333 min).

4.2.13. (E)-1-(2-Naphthyl)-3-(4-pyridyl)prop-2-en-1-one (6m, DMU780) Method 3; Yellow solid (39%). mp 126-127°C; ^{1}H NMR ($CDCl_3$): δ 7.51 (2H, d, *J* = 6.1 Hz), 7.54-7.68 (2H, m), 7.75 (1H, d, *J* = 15.3 Hz), 7.83 (1H, d, *J* = 15.3 Hz), 7.90 (1H, d, *J* = 7.6 Hz), 7.96 (1H, d, *J* = 8.3 Hz), 8.00 (1H, d, *J* = 8.3 Hz), 8.09 (1H, dd, *J* = 1.0, 9.7 Hz), 8.54 (1H, s), 8.72 (1H, d, *J* = 6.1 Hz); ^{13}C NMR ($CDCl_3$): δ 122.07, 124.30, 126.09, 127.01, 127.91, 128.77, 128.85, 129.60, 130.32, 132.53, 134.90, 135.72, 141.47, 142.17, 150.69, 189.54; IR (KBr) /cm^{-1} 1663 (C=O); HRMS found [M]+ 260.1071, $C_{18}H_{13}NO$ requires [M]+ 260.1070; Purity 97 % HPLC (Retention time 9.835 min).

4.2.14. (E)-1-(3-Phenanthrenyl)-3-(3-pyridinyl) prop-2-en-1-one (6n, DMU2136) Method 2; Bright yellow solid (61%). mp 113-114°C; ^{1}H NMR ($CDCl_3$): δ 7.38 (1H, dd, *J* = 5.8, 7.1 Hz), 7.61-8.00 (9H, m), 8.19 (1H, dd, *J* = 5.8, 1.3 Hz), 8.67 (1H, d, *J* = 7.1 Hz), 8.91 (1H, d, *J* = 1.2 Hz), 9.35 (1H, s); ^{13}C NMR ($CDCl_3$): δ 122.78, 123.81, 124.06, 124.14, 125.62, 126.30, 127.30, 127.37, 128.89, 129.08, 129.87, 129.93, 130.61, 130.78, 132.23, 134.68, 135.05, 135.44, 140.99, 147.13, 151.07, 150.17, 189.74; IR (KBr) /cm^{-1} 1655 (C=O); HRMS found [M]+ 310.1230, $C_{22}H_{15}NO$ requires [M]+ 310.1226; Purity 96 % HPLC (Retention time 17.154 min).

4.2.15. (E)-1-(9-Phenanthrenyl)-3-(3-pyridinyl)prop-2-en-1-one (6o, DMU2137) Synthetic Method 2; Yellow solid (61%). mp 120-121°C; ^{1}H NMR ($CDCl_3$): δ 7.15 (1H, dd, *J* = 4.8, 9.1 Hz), 7.42 (1H, d, *J* = 15.2 Hz), 7.62-7.79 (5H, m), 7.90-7.99 (2H, m), 8.05 (1H, s), 8.34 (1H, dd, *J* = 1.0, 8.6 Hz), 8.63 (1H, dd, *J* = 4.8, 1.1 Hz), 8.72 (1H, d, *J* = 8.6 Hz),

8.77 (1H, d, *J* = 8.6 Hz), 8.80 (1H, d, *J* = 1.5 Hz); ^{13}C NMR ($CDCl_3$): δ 122.79, 123.05, 123.82, 126.45, 127.25, 127.35, 127.45, 128.68, 128.74, 128.82, 129.13, 129.69, 130.10, 130.43, 130.82, 131.64, 134.54, 135.57, 142.04, 150.17, 151.35, 194.94; IR (KBr) /cm^{-1} 1651 (C=O); HRMS found [M]+ 310.1228, $C_{22}H_{15}NO$ requires [M]+ 310.1226; Purity >99 % HPLC (Retention time 17.366 min).

4.2.16. (E)-1-(1-Pyrenyl)-3-(3-pyridyl)prop-2-en-1-one (6p, DMU2140) Method 2; Bright yellow solid (54%). mp 113-114°C; ^{1}H NMR ($CDCl_3$): δ 7.33 (1H, dd, *J* = 4.8, 8.0 Hz), 7.53 (1H, d, *J* = 16.1 Hz), 7.65 (1H, d, *J* = 16.1 Hz), 7.89-7.93 (1H, m), 8.03-8.11 (2H, m), 8.15-8.28 (6H, m), 8.61 (1H, dd, *J* = 1.6, 4.8 Hz), 8.64 (1H, d, *J* = 8.8 Hz), 8.89 (1H, d, *J* = 1.6 Hz); ^{13}C NMR ($CDCl_3$): δ 123.82, 124.09, 124.39, 124.58, 124.97, 126.14, 126.32, 126.34, 126.50, 127.18, 129.07, 129.40, 129.58, 130.55, 131.15, 133.59, 134.51, 141.76, 150.13, 151.25, 194.96; IR (KBr) /cm^{-1} 1620 (C=O); HRMS found [M]+ 334.1227, $C_{24}H_{15}NO$ requires [M]+ 334.1226; Purity >99 % HPLC (Retention time 19.736 min).

4.2.17. (E)-3-(3-Hydroxyphenyl)1-(3-pyridyl)prop-2-en-1-one (7a, DMU767) Method 3; Yellow solid (17%). mp 192-193°C; ^{1}H NMR (DMSO-d_6): δ 6.92 (1H, d, *J* = 8.0 Hz), 7.24-7.35 (3H, m), 7.62 (1H, dd, *J* = 7.6, 5.6 Hz), 7.68 (1H, d, *J* = 16.0 Hz), 7.84 (1H, d, *J* = 16.0 Hz), 8.44-8.48 (1H, m), 8.81 (1H, dd, *J* = 1.0, 5.6 Hz), 9.29 (1H, d, *J* = 1.2 Hz), 9.78 (1H, brs); ^{13}C NMR (DMSO-d_6) δ 115.39,118.15, 120.08, 121.66, 123.93, 129.90, 132.81, 135.70, 135.97, 145.05, 149.55, 153.35, 157.72, 188.57; IR (KBr) /cm^{-1} 1662 (C=O); HRMS found $[M+1]^+$ 226.0863, $C_{14}H_{11}O_2N$ requires $[M+1]^+$ 226.0863; HPLC purity 98 % (Retention time 3.947 min).

4.2.18. (E)-3-(3,4-Methylenedioxyphenyl)-1-(3-pyridyl)prop-2-en-1-one (7b, DMU769) Method 2; Yellow solid (76%). mp 144-145°C; ^{1}H NMR (DMSO-d_6): δ 6.11 (2H, s), 7.01

(1H, d, *J* = 8.5 Hz), 7.36 (1H, dd, *J* = 1.1, 8.5 Hz), 7.62 (1H, dd, *J* = 8.5, 4.8 Hz), 7.67 (1H, d *J* = 1.1 Hz), 7.73 (1H, d, *J* = 15.4 Hz), 7.82 (1H, d, *J* = 15.4 Hz), 8.44-8.48 (1H, m), 8.82 (1H, dd, *J* = 4.8, 1.6 Hz), 9.31 (1H, d, *J* = 1.1 Hz); ^{13}C NMR (DMSO-d_6) δ 101.70, 107.02, 108.55, 119.67, 123.91, 126.39, 128.95, 133.94, 135.87, 144.83, 146.63, 148.11, 149.55, 153.15, 188.19; IR (KBr) /cm^{-1} 1662 (C=O); HRMS found $[M+1]^+$ 254.0812, $C_{15}H_{12}O_3N$ requires $[M+1]^+$ 254.0823; HPLC purity 97 % (Retention time 5.681 min).

4.2.19. (E)-3-(3-Methoxyphenyl)-1-(3-pyridyl)prop-2-en-1-one (7c, DMU789) Method 2; Light brown solid (33%). mp 78-79°C; ^{1}H NMR ($CDCl_3$): δ 3.87 (3H, s), 6.99 (1H, dd, *J* = 8.4, 2.4 Hz), 7.14-7.19 (1H, m), 7.25 (1H, d, *J* = 6.6 Hz), 7.36 (1H, t, *J* = 6.6 Hz), 7.44-7.50 (2H, m), 7.80 (1H, d, *J* = 15.5 Hz), 8.26-8.31 (2H, m), 8.81 (1H, dd, *J* = 1.2, 5.4 Hz), 9.23 (1H, d, *J* = 1.1 Hz); ^{13}C NMR ($CDCl_3$): δ 55.39, 113.57, 116.18, 121.28, 121.74, 123.69, 130.08, 133.51, 135.83, 145.96, 149.79, 153.21, 160.04, 189.18; IR (KBr) /cm^{-1} 1662 (C=O); HRMS found $[M+1]^+$ 240.1017, $C_{15}H_{13}O_2N$ requires $[M+1]^+$ 240.1019; Purity >99 % HPLC (Retention time 6.641 min).

4.2.20. (E)-3-(2-Methoxyphenyl)-1-(3-pyridyl)prop-2-en-1-one (7d, DMU790) Method 2; Yellow solid (50%). mp 95-96°C; ^{1}H NMR (DMSO-d_6): δ 3.90 (3H, s), 7.04 (1H, t, *J* = 8.1 Hz), 7.13 (1H, d, *J* = 7.6 Hz), 7.44-7.51 (1H, m), 7.60 (1H, dd, *J* = 4.9, 7.6 Hz), 7.88 (1H, d, *J* = 16.3 Hz), 8.00 (1H, dd, *J* = 1.6, 7.6 Hz), 8.10 (1H, d, *J* = 16.3 Hz), 8.41-8.47 (1H, m), 8.82 (1H, dd, *J* = 1.6, 4.9 Hz), 9.28 (1H, d, *J* = 2.2 Hz); ^{13}C NMR (DMSO-d_6) δ 55.74, 111.83, 120.72, 121.52, 122.63, 123.95, 128.61, 132.70, 134.94, 135.90, 149.48, 153.19, 158.39, 188.60; IR (KBr) /cm^{-1} 1663 (C=O); HRMS found $[M+1]^+$ 240.1019, $C_{15}H_{13}O_2N$ requires $[M+1]^+$ 240.1019; Purity >99 % HPLC (Retention time 7.154 min).

4.2.21. (E)-3-(3-Hydroxy-4-methoxyphenyl)-1-(3-pyridyl)prop-2-en-l-one (7e, DMU2103) Method 3; Bright yellow solid (13%). mp 157-158°C; ^{1}H NMR (DMSO-d_6): δ 3.85 (3H, s), 7.12 (1H, d, *J* = 7.4 Hz), 7.30-7.35 (2H, m), 7.60 (1H, dd, *J* = 5.1, 7.4 Hz), 7.63-7.74 (2H, m), 8.41-8.46 (1H, m), 8.81 (1H, dd, *J* = 5.1, 0.9 Hz), 9.23 (1H, s), 9.28 (1H, d, *J* = 1.1 Hz); ^{13}C NMR (DMSO-d_6) δ 55.68, 111.90, 114.95, 119.17, 122.50, 123.90, 127.14, 134.94, 135.85, 145.35, 146.63, 149.44, 150.61, 153.04, 188.29; (C=O); IR (KBr) /cm^{-1} 1658 (C=O); HRMS found $[M+1]^+$ 256.0970, $C_{15}H_{13}O_3N$ requires $[M+1]^+$ 256.0968; Purity >99 % HPLC (Retention time 4.950 min).

4.2.22. (E)-3-(3, 4-Dimethoxyphenyl)-1-(3-pyridyl) prop-2-en-1-one (7f, DMU774) Method 3; Yellow solid (15%). mp 88-89°C; ^{1}H NMR (DMSO-d_6): δ 3.81 (3H, s), 3.85 (3H, s), 7.04 (1H, d, *J* = 9.3 Hz), 7.40 (1H, dd, *J* = 9.8, 1.6 Hz), 7.56 (1H, d, *J* = 1.6 Hz), 7.59 (1H, dd, *J* = 4.7, 8.8 Hz), 7.74 (1H, d, *J* = 15.5 Hz), 7.84 (1H, d, *J* = 15.5 Hz), 8.41-8.46 (1H, m), 8.81 (1H, dd, *J* = 1.0, 4.7 Hz), 9.14 (1H, d, *J* = 1.5 Hz); ^{13}C NMR (DMSO-d_6) δ 56.00, 110.78, 111.55, 119.31, 123.89, 124.43, 127.14, 133.05, 135.82, 145.31, 149.03, 149.60, 151.51, 151.56, 153.13, 188.20; IR (KBr) /cm^{-1} 1658 (C=O); HRMS found $[M+1]^+$ 270.1126, $C_{16}H_{15}O_3N$ requires $[M+1]^+$ 270.1125; Purity 99 % HPLC (Retention time 5.852 min).

4.2.23. (E)-1-(3-Pyridyl)-3-(3, 4, 5-trimethoxyphenyl)prop-2-en-1-one (7g, DMU2114)[60] Method 2; Bright yellow solid (37%). mp 123-124°C; ^{1}H NMR (DMSO-d_6): δ 7.24 (3H, s), 7.62 (1H, dd, *J* = 7.2, 4.8 Hz), 7.75 (1H, d, *J* = 16.1 Hz), 7.90 (1H, d, *J* = 16.1 Hz), 8.43-8.48m (1H, m), 8.83 (1H, dd, *J* = 4.8, 1.6 Hz), 9.36 (1H, d, *J* = 1.2 Hz); ^{13}C NMR (DMSO-d_6) δ 60.13, 106.73, 120.93, 123.93, 129.94, 132.88, 135.91, 140.00, 145.27, 149.64, 153.08, 153.23, 188.36; IR (KBr) /cm^{-1} 1662 (C=O); HRMS found $[M+1]^+$ 300.1231, $C_{17}H_{17}O_4N$ requires $[M+1]^+$ 300.1230; HPLC purity >99 % (Retention time 5.403 min).

4.2.24. (E)-1-(3-Pyridyl)-3-(2, 3, 4-trimethoxyphenyl) prop-2-en-l-one (7h, DMU2117) Method 2; Bright yellow solid (57%). mp 78-79°C; ^{1}H NMR (DMSO-d_6): δ 3.78 (3H, s), 3.88 (6H, s), 6.94 (1H, d, *J* = 9.3 Hz), 7.60 (1H, dd, *J* = 5.2, 7.8 Hz), 7.83 (1H, d, *J* = 9.3 Hz), 7.83 (1H, d, *J* = 15.6 Hz), 7.96 (1H, d, *J* = 15.6 Hz), 8.40-8.46 (1H, m), 8.82 (1H, dd, *J* = 5.2, 1.1 Hz), 9.29 (1H, d, *J* = 1.1 Hz); ^{13}C NMR (DMSO-d_6) δ 56.07, 60.43, 61.55, 108.48, 120.12, 120.73, 123.58, 128.87, 133.06, 135.79, 139.14,141.70, 149.48, 153.10, 153.23, 156.06, 188.34; IR (KBr) /cm^{-1} 1658 (C=O); HRMS found $[M+1]^+$ 300.1230, $C_{17}H_{17}O_4N$ requires $[M+1]^+$ 300.1230; Purity 98 % HPLC (Retention time 5.583 min).

4.2.25. (E) 3-(3, 4-Dichlorophenyl)-1-(3-pyridyl)prop-2-en-1-one (7i, DMU778) Method 2; Yellow solid (70%). mp 168-169°C; ^{1}H NMR (DMSO-d_6): δ 7.61 (1H, dd, *J* = 7.7, 5.1 Hz), 7.72 (1H, d, *J* = 9.2 Hz), 7.75 (1H, d, *J* = 15.4 Hz), 7.89 (1H, dd, *J* = 9.2, 1.5 Hz), 8.06 (1H, d, *J* = 15.4 Hz), 8.44-8.50 (1H, m), 8.83 (1H, dd, *J* = 1.5, 5.1 Hz),m 9.35 (1H, d, *J* = 1.5 Hz); ^{13}C NMR (DMSO-d_6) δ 123.78, 123.95, 129.33, 130.31, 131.02, 131.84, 132.52, 132.99, 135.34, 136.03, 141.84, 149.82, 153.51, 188.26; IR (KBr) /cm^{-1} 1670 (C=O); HRMS found $[M+1]^+$ 279.0171, $C_{14}H_9ONCl_2$ requires $[M+1]^+$ 279.0168; Purity >99 % HPLC (Retention time 9.740 min).

4.2.26. (E) 3-(3, 4-Difuorophenyl)-1-(3-pyridyl)prop-2-en-1-one (7j, DMU2101) Method 2; Off-white solid (13%). mp 135-136°C; ^{1}H NMR (DMSO-d_6): δ 7.49-7.58 (1H, m), 7.60 (1H, dd, *J* = 5.0, 8.5 Hz), 7.71-7.79 (2H, m), 7.98 (1H, d, *J* = 15.0 Hz), 8.10-8.15 (1H, m), 8.42-8.49 (1H, m), 8.82 (1H, dd, *J* = 1.5, 5.0 Hz), 9.33 (1H, d, *J* = 1.5 Hz); ^{13}C NMR (DMSO-d_6) δ 117.07, 117.25, 117.91, 118.08, 122.97, 122.99, 123.94, 127.03, 127.10, 132.57, 135.97, 142.35, 149.75, 153.45, 188.22; IR (KBr) /cm^{-1} 1670 (C=O); HRMS found

$[M+1]^+$ 246.0728, $C_{14}H_9ONF_2$ requires $[M+1]^+$ 246.0725; Purity 97 % HPLC (Retention time 6.723 min).

4.2.27. (E)-3-(2-Naphthyl)-1-(3-pyridyl)prop-2-en-1-one (7k, DMU2105) Method 3; Yellow solid (29%). mp 136-137°C; ^{1}H NMR ($CDCl_3$): δ 7.47 (1H, dd, *J* = 5.2, 7.5 Hz), 7.50-7.56 (2H, m), 7.60 (1H, d, *J* = 16.3 Hz), 7.80 (1H, dd, *J* = 9.3, 1.3 Hz), 7.84-7.93 (3H, m), 8.03 (1H, d, *J* = 16.3 Hz), 8.06 (1H, s), 8.30-8.35 (1H, m), 8.82 (1H, dd, *J* = 5.2, 1.3 Hz), 9.28 (1H, d, *J* = 1.2 Hz); ^{13}C NMR ($CDCl_3$): δ 121.50, 123.56, 123.70, 126.92, 127.67, 127.87, 128.75, 128.92, 131.17, 131.97, 133.35, 133.63, 134.61, 135.92, 146.12, 149.81, 153.20, 189.12; IR (KBr) /cm^{-1} 1654 (C=O); HRMS found $[M+1]^+$ 260.1073, $C_{18}H_{13}ON$ requires $[M+1]^+$ 260.1070; HPLC purity >99 % (Retention time 9.269 min).

4.2.28. (E)-3-phenyl-1-(3-pyridyl)prop-2-en-1-one (7l, DMU2118) Method 2; Yellow solid (29%). mp 79-80°C; ^{1}H NMR ($CDCl_3$): δ 7.41-7.52 (5H, m), 7.62-7.69 (2H, m), 7.85 (1H, d, *J* = 15.0 Hz), 8.26-8.31 (1H, m), 8.80 (1H, dd, *J* = 4.5, 1.3 Hz), 9.24 (1H, d, *J* = 1.8 Hz); ^{13}C NMR ($CDCl_3$): δ 121.43, 123.69, 128.64, 129.09, 131.02, 133.54, 134.47, 135.91, 146.04, 149.78, 153.19, 189.17; IR (KBr) /cm^{-1} 1666 (C=O); HRMS found $[M+1]^+$ 210.0913, $C_{14}H_{11}ON$ requires $[M+1]^+$ 210.0913; Purity >99 % HPLC (Retention time 6.255 min).

4.3. Biology protocols

4.3.1. Plasmid constructs. All plasmids were constructed using standard molecular biological techniques. The primers used for isolation of the human *CYP1B1* coding sequence from a human liver cDNA library were:

5’ GGATCCAAAAAAATGCTCAGCCCGAACGACCCTTGG 3’ (forward primer) and

5’ TCTAGATTATTGGCAAGTTTCCTTGGCTTGTAAATTTTG 3’ (reverse primer).

The primers used for isolation of the yeast *GAL1* promoter from a yeast genomic library created from the strain S288C were:

5' AAGCTTGATATCGAATTCCTTGAATTTTCAAAAATTCTTAC 3' (forward primer), and 5' GGATCCGGGGTTTTTTCTCCTTGACGTTAAAGTATAGAGG 3' (reverse primer).

The polymerase that was used for amplification of DNA sequences was Pfu (Promega).

4.3.2. Yeast transformation. Yeast plasmids were introduced into the yeast strain YY7 which is W303 Matα that contains the human reductase gene integrated in the yeast cells' *LEU2* chromosomal loci, using standard transformation protocols.[61]

4.3.3. Selection of a high CYP1B1-producing yeast strain. Fifty colonies (each of them representing a potential CYP1B1-producing recombinant yeast strain), obtained after transforming the plasmid pSYE225 (encoding the human *CYP1B1* gene) in the yeast strain YY7, were grown in 1 ml minimal medium SD [6.7g yeast nitrogen base (Becton Dickinson)/L, 20g glucose (Sigma)/L, with required supplementation for auxotrophic markers] in sterile 6-well plastic plates, for 24h, at 30°C at 220 rpm.

For CYP1B1 enzyme expression, cells were inoculated from an SD pre-culture into fresh 1 ml YPGE medium [10g yeast extract (Oxoid)/L, 10g protease peptone (Oxoid)/L, 20g/L glucose, 30ml pure ethanol (Sigma-Aldrich)/L] that allows full induction of the *GAL1* promoter. 0.4 ml of 50% galactose was added after 16h. The cells were grown for another 16h, before further analyses.

~1x 10^7 cells were aliquoted into microfuge tubes and the cells were spun down in a bench-top microfuge for 30 sec at 13,000 rpm. The supernatant was removed carefully and the

pellet was re-suspended in 1 ml TE(50mM Tris, pH 7.4; 1mM EDTA; pH 7.5). This was repeated two more times and the cells were finally re-suspended in 0.2 ml TE.

50 µl of the resulting cell suspension was transferred into a clear flat-bottomed 96-well plate for the addition of 50 µl of a substrate solution that contains 7-ethoxyresorufin (7-ER; Sigma-Aldrich), the CYP1B1 substrate. The final concentration of 7-ER in the 100 µl cellular mixture was 5 µM and the concentration of DMSO 0.5%.

The assay (monitoring the conversion of 7-ER to resorufin, mediated by cellular CYP1B1) was performed using a Synergy HT Biotek plate reader. The plate reader was set up to shake the plate for 5 sec at medium intensity (setting of 4) between each reading. The temperature of the plate was kept at 30°C. The fluorescence of the product formed was monitored over a period of 40 min. Fluorescence was measured at 571/585 nm (excitation/emission maximum) using a filter that can monitor such fluorescence excitation/emission. The strain that emitted the highest fluorescence was chosen for preparation of microsomes.

4.3.4. Preparation of *Sacchrosomes*

Yeast cell culture. The best CYP1B1-producing yeast strain was inoculated as a single colony from a SD minimal medium agar plate into 10 ml of YPD culture broth [10g/L yeast extract, 20 g/L proteose peptone] in a 100 ml conical flask. The pre-culture was shaken at 220 rpm for 18 h, at 30 °C.

1 ml of the pre-culture was inoculated into SW6 medium [750 ml minimal medium (without glucose)/L, 1g casein hydrolysate (Sigma)/L, 20g/L glucose + auxotrophic complement of nucleosides required by the strain]. The culture was shaken at 220 rpm for 18h, at 30°C.

~4x 10^7 cells from the culture grown in SW6 medium were inoculated into 400 ml of YPGE medium in a 2L conical flask. The culture was shaken at 220 rpm for 16h, at 30°C and then galactose was added so that the final concentration was 2%.Addition of galactose induced the expression of CYP1B1.The culture was again shaken at 30°C for 16h, after which 8g of galctose was added, cells incubated at 30°C for another 16h and then the cells were centrifuged.

Preparation of CYP1B1-Sacchrosomes. The procedure has largely been modified from what has been published.[62] The cell pellet was re-suspended in cold DMB-A buffer [10 mM Tris-HCl, pH 7.6, 0.1 mM EDTA, pH 8, 65 mM Sorbitol, 2.66 mM AEBSF (4-(2 aminoethyl)benzenesulfonylfluoride.HCl; Melford), 0.266 mM DTT (dithiothreitol; Melford)]; AEBSF (Sigma) is a protease inhibitor. Per gram of wet cell weight, 50 ml of DMB-A buffer was used for re-suspension. The re-suspended cells were kept on ice and all procedures henceforth were performed on ice.

The outer cell wall of the re-suspended yeast cells was disrupted in a cell disruptor (Constant Systems Basic Z model with continuous flow head fitted disruptor) using a pressure of 22.5 kilopound per square inch (ksi).The disrupted cells were centrifuged for 15 min at 4500 rpm at 4°C using a Sorvall bench top centrifuge. After this, the resultant supernatant was subjected to three consecutive centrifugations at 17,000 rpm (on a Beckman Coulter centrifuge); each centrifugation was conducted at 4°C for 20 minutes and each time the supernatants were collected. After the third centrifugation, the supernatant, on ice, was diluted with ice-cold DMB-TES buffer [50 mM Tris-HCl, pH 7.6, 1 mM EDTA, pH 8, 600 mM Sorbitol, 2.66 mM AEBSF, 0.266 mM DTT] and 0.125MNaCl was added.

For precipitation of Sacchrosomes, cold 50% PEG (w/v) was added drop-wise to the diluted supernatant and the mixture was kept on ice for 30 min before it was centrifuged at 12,000 g (on a Beckman Coulter Avanti J-20 XP centrifuge) for 20 min. After centrifugation, the supernatant was discarded and the pellets are the CYP1B1-Sacchrosomes. They were rinsed twice with 5 ml DMB-B buffer (10 mM Tris-HCl, 1 mM EDTA and 20 % Glycerol) and after that it was gently re-suspended in DMB-B buffer (volume used depended on the size of pellet) using a Teflon homogeniser (Fisher, catalogue no. FP56691).

Once the Sacchrosomes were prepared, protein concentrations were determined using the Bradford assay following the instructions of the manufacturer (Bio-Rad).

An identical procedure was followed to prepare the Sacchrosomes that contained no enzyme and those that contained CYP1A1, CYP1A2, CYP3A4 and CYP2D6.

4.3.5. Determination of CYP450 content. The actual amount of CYP450s was determined using CO-difference spectroscopy.[63]

4.3.6. Inhibition of CYP450 Sacchrosomes and IC_{50} determination. Percentage inhibition was determined at a particular concentration of the compound which is usually 10 µM. The compounds that inhibited the best at 10 µM concentrations were chosen for determination of IC_{50} values (the concentration at which 50% of the enzyme activity is inhibited). Both percentage inhibition and IC_{50} values effectively reflect the inhibitory potential of a compound and hint at the possible effectiveness of a compound in a biological process.

An assay which determines IC_{50} values includes the Sacchrosomes^{TM} (i.e. CYP450-bearing yeast microsomes), a chosen chemical compound in six serial dilutions in DMSO (with DMSO concentration never exceeding 0.5%), 96-well flat-bottomed microtitre plate, substrates such as ER (7-ethoxyresorufin) or CEC (3-cyano-7-ethoxycoumarin) or EOMCC

(7-ethoxy-methyloxy-3-cyanocoumarin) or DBF (dibenzylfluorescein), depending on the CYP450 used in the assay.[64] The substrates form fluorescent compounds upon CYP metabolism.A fluorescent plate reader is used to monitor fluorescence emitted which ultimately determines IC_{50} values via measurement of fluorescence units at each endpoint (i.e. at each concentration of compound used).

4.3.7. End point assays for inhibition of Sacchrosomes. *A typical inhibition assay for CYP1B1 in Sacchrosomes*. Regenerating system consists of:5 µl Solution A (183 mg of $NADP^+$ + 183 mg of glucose-6-phosphate + 654 µl of 1.0 M magnesium chloride solution + 9.15 ml of sterile ultra-pure water) + 1 µl Solution B (250 Units of glucose-6-phosphate dehydrogenase + 6.25 ml of 5 mM sodium citrate; mixed in a tube and made up to 10 ml with sterile ultra-pure water) + 39 µl 0.2 M phosphate buffer (KPi; 0.6 ml of 1.0M K_2HPO_4 + 9.4 ml of 1.0M KH_2PO_4 mixed and made up to 50 ml with sterile ultra-pure water) + 5 µl potential inhibitory compound.

Enzyme system consists of: 0.5 µl CYP1B1 (0.5 pmoles) + 1.7 µl control protein (denatured proteins from yeast cells that do not contain recombinant CYP450 proteins) + 5 µl 0.1 mM 7-ER (7-ethoxyresorufin substrate) + 42.8 µl 0.1M Kpi (0.3 ml of 1.0 M K_2HPO_4 + 4.7 ml of 1.0 M KH_2PO_4 were mixed and made up to 50 ml with sterile ultra-pure water.

The assay is performed using (a) sensitivity (Gain): 65/70/75 of the Biotek Synergy plate reader (this would differ from one instrument to the other) and (b) Filter: 530/590 nm that monitors fluorescence excitation/ emission of resorufin, the metabolite of 7-ethoxyresorufin substrate (ER); the excitation/ emission differs with the substrate that is used.

Similar assays were performed with Sacchrosomes^{TM} bearing the other human CYP enzymes using appropriate fluorescent substrates, as detailed above.

4.3.8. Determination of IC_{50} values using Sacchrosomes™. The plate reader (BioTek) was warmed at 37 °C. Compounds were serially diluted to six different concentrations with 10%DMSO in a Sero-Wel white microplate. Serial dilutions were made with a dilution factor of 1: 20. 45 µl of regenerating system was prepared and pre-warmed at 37 °C, as detailed in Table 4. Meanwhile, 50 µl of enzyme substrate mix reaction was prepared and incubated at 37 °C for 10 min (Table 5).

Table 4.

Table 5.

In wells of a black 96-well flat-bottomed microplate, 45 µl of regenerating system, 5 µl serial dilutions of inhibitor were pipetted out from the dilution plate and then 50 µl of enzyme/substrate was added except in control well (positive control); for this well, instead of inhibitor 5 µl of 10%DMSO was added. In the background well (negative control), only 45 µl regeneratingsystem and 5 µl 10% DMSO were added with no enzyme; the microplate was then vortexed for a few seconds. The microplate was incubated for 10 min. which was followed by addition of 75 µl of Tris-acetonitrile to all wells, using an eight-channel multi-pipette, to stop the reaction; after that 50 µl of enzyme/substrate reaction was added into the 'negative control' well. The plate was left to shake for 10 sec and the fluorescence units for each endpoint were monitored at appropriate settings (for assay parameters and plate layout) selected on the KC4 software of the BioTek plate reader.

Calculation of IC_{50} values. To calculate IC_{50} values, a series of dose-response data, for example, drug concentrations (x_1, x_2, ...,x_n) at which specific growth inhibition occurs (y_1, y_2, ...,y_n) were generated. The values of y were in the range of 0-1.

The simplest estimate of IC_{50} is to plot x-y and fit the data with a straight line (via linear regression). IC_{50} values are then estimated using the fitted line, i.e.

$Y = a * X + b,$

$IC_{50} = (0.5 - b)/a.$

Raw data was imported and computed in Microsoft Excel. The maximum change in relative fluorescence units (RFU) relative to positive control with 0.5% DMSO was calculated. The enzyme inhibition was plotted using sigmoidal curve (4 parameter variable slope equation) and half inhibitory concentration (IC_{50}) values were analysed statistically using Graph-Pad Prism Software (Version 6.0) using Prism's statistical software.

4.3.9. Growth of yeast strains for determination of IC_{50} values for CYP1B1 enzyme inhibition in live yeast cells. The yeast strain, harbouring the human *CYP1B1* gene expression cassette, was streaked out from a glycerol stock and grown on SD-minimal medium agar plates with the required supplements, at 30 ºC for 3 days. Single colonies were then picked and grown, at first, as pre-cultures in minimal medium and then grown in full YP-Gal medium [10g yeast extract (Oxoid)/L, 10g protease peptone (Oxoid)/L, 20g/L galactose] for expression of the CYP1B1 enzyme.

4.3.10. Determination of IC_{50} values using recombinant yeast live cells, grown in suspension. For IC_{50} determinations, 4×10^8 cells (equivalent to approximately 25 OD_{600}) were taken from the exponential growth phase, approximately 16-20 h after induction of CYP1B1 protein. These cells, enough for 100 assays, were aliquoted appropriately into eppendorf tubes. Cells were centrifuged on a bench top microfuge for 30 sec at 13,000 rpm (15.7 g). The supernatants were removed carefully so as to not dislodge the pellet. The cell pellets were then re-suspended in 650 µl of TE buffer (50 mMTris-HClpH. 7.4, 1 mM

EDTA). The cells were diluted 1:10 before carrying out an IC_{50} determination using a protocol similar to the determination of IC_{50}s in Sacchrosomes™. IC_{50} values were calculated as described above using Graph-Pad Prism Software (Version 6.0) using Prism's statistical software.

4.3.11. Cell lines used for this study. The adherent cell lines used in this study, HEK293, A2780 and A2780cis, were obtained from ECACC. They were tested and authenticated via (a) short tandem repeat (STR) profiling, (b) monitoring of cell morphology, (c) karyotyping, and (d) cytochrome C oxidase I (COI) assay by ECACC before purchase of cell lines. The cell lines were revived immediately after receipt.

4.3.12. Transfection of mammalian expression plasmid that encodes human *CYP1B1*gene, isolated from a human liver cDNA library, in HEK293 cells, grown in suspension cells. HEK293 'suspension' cells (1 x 10^6 per mL),adapted for growth in suspension form adherent HEK293 cells (ECACC catalogue no 85120602)were obtained from CYP Design Ltd. Cells were counted using improved Neubauer counting chamber and the cell viability (≥ 90% viability) was determined using trypan blue dye exclusion. Actively dividing suspension cells in log phase were seeded in appropriate volumes in Erlenmeyer flask (Corning #431143) and incubated at 37 °C, 8% CO_2 and shaken at 130 rpm on an orbital shaker (Panasonic). Before transfection, the mammalian expression plasmids(pcDNA3.1/CYP1B1 and pcDNA3.1/CYP1A1) containing human *CYP1A1* and *CYP1B1* genes (isolated from a human liver cDNA library) were propagated in *E. coli*DH5α, grown in LB medium in presence of ampicillin (50 µg/mL).The endotoxin-free plasmids were prepared using Zymo PURE™ Plasmid Maxiprep Kit as per manufacturer's instructions (#D4202, Zymo Pure). The quantity and purity of plasmid DNA ($A_{260/280}$ ≥ 1.9) was

determined by Bio Spectrophotometer (Eppendorf). The quality of plasmids DNA was determined using 1% agarose gel electrophoresis.

To initiate transfection, the respective plasmid DNA – cationic lipid complexes were prepared as per manufacturer's instructions (Invitrogen #16447-100) in OptiPRO SFM reduced serum medium (Invitrogen #12309-09). Further, the aseptic preparation of DNA-lipid complexes was added slowly to the respective flasks containing HEK293 suspension cells. The negative control was prepared by adding OptiPRO SFM reduced serum media without plasmid DNA. The suspension cells were incubated at 37 °C and checked for optimal expression of CYP enzymes at regular intervals. 24 to 48 h post transfection, the cells were counted and the cell viability was determined. The transfected cells in sufficient volumes were spun at 200 x g for 5 minutes. The supernatant was discarded and the cells were washed once with pre-warmed phosphate buffered saline. The cells were once again spun at 200 x g for 5 min at room temperature and the supernatant was discarded. The cells were gently re-suspended in pre-warmed growth media to obtain cell density 4 x 10^6 cells per mL for CYP1B1 and 2 x 10^6 cells per mL for CYP1A1 transfected HEK293 cells, respectively.

4.3.13. Screening of potential CYP inhibitors using recombinant human live HEK293cells, grown in suspension. For screening of potential compounds, recombinant HEK293 cells (100 - 200 x 10^3 cells per well) expressing CYP enzymes were seeded in 50 µL volume in triplicates in black 96-well plates with transparent bottom (Corning #3904). The test compounds either at single point concentrations (10 µM) or at various concentrations (ranging from 1 nM to 30 µM) for determination of IC_{50}values were added in 25 µL volume to the wells followed by incubation at 37°C, 8% CO_2 for 30 min. After incubation, the fluorogenic substrate 7-ethoxyresorufin was added at 5 µM in 25 µL to the wells and contents were mixed homogenously by shaking to perform the 7-ethoxyresorufin-O-deethylase

(EROD) assay. The plate was read on a 96 well plate-reader (Biotek, Synergy HT) for 60 min using suitable wavelengths for emission (530/30) and excitation (590/40) of fluorescence. IC_{50} values were calculated as described above using Graph-Pad Prism Software (Version 6.0) using Prism's statistical software.

4.3.14. A2780cis cells, resistant to cisplatin, overproduce CYP1B1. The cisplatin-sensitive ovarian cancer cell line A2780 (catalogue no 93112519) and the corresponding cisplatin-resistant line A2780cis (catalogue no 93112517), developed via chronic exposure to cisplatin, were obtained from ECACC. Both A2780 and A2780cis cells were cultured in RPMI-1640 medium (Lonza, BE12-167F) supplemented with 0.2 mM L-glutamine (Invitrogen, 25030024), 10% heat-inactivated foetal bovine serum (FBS; Sigma, F6178), 1% penicillin-streptomycin solution; the cisplatin-resistant line was cultured in the presence of 1 μM cisplatin (Sigma, P4394), as suggested by ECACC.

Western blotting was performed following standard protocols and following the instructions provided by Bio-Rad. After probing the blots with primary and secondary antibodies, the proteins were detected by chemiluminescence using the ECL kit (Abcam, Cat. No. Ab65623) and the Gel Doc system (Bio Rad).

4.3.15. Restoration of cisplatin-sensitivity to HEK293 and A2780 cells that overexpress CYP1B1. HEK293 cells were cultured in RPMI1640 without L-glutamine (Lonza, BE12-167F) supplemented with 4 mM L-glutamine (Invitrogen, 25030024), 10% heat-inactivated foetal bovine serum (FBS; Sigma, F6178), 1% non-essential amino acids (Sigma, M7145) and 1% penicillin-streptomycin solution (Invitrogen, 15140-122). A2780 cells were cultured as described above.

Endotoxin-free plasmids used for transfection were purified using columns (Qiagen). Plasmids were transfected using the AmaxaNucleofector^{TM} (Lonza) following the protocols published by Lonza on the web. Usually, 1x 10^6 cells were transfected with 1.5 µg of DNA. After transfection, cells were expanded in the presence of the antibiotic G418; transfected cells bearing the plasmid would be resistant to G418. Western blot was performed as described above.

Transfected and non-transfected cells (~1×10^3) were seeded in a 96-well plate with different concentrations of cisplatin, in triplicates. Enzyme inhibition studies were carried out by co-administering at 10x IC_{50} concentrations, in the cell culture medium, DMU2105 and DMU2139, two of the most potent inhibitors of CYP1B1 and ANF (the known CYP1B1 inhibitor). The MTT assay was performed using HEK293 and 2780 cells, transfected with pcDNA3.1/CYP1B1, pcDNA3.1 using protocols published earlier.[65, 66]

Each experiment was performed three times.

4.3.16. Molecular modelling with panel of CYP enzymes. The human CYP family of enzymes are oxidoreductases involved in the metabolism of xenobiotics, mainly hydroxylation of unreactive carbon atoms in aromatic and aliphatic rings or aliphatic chains. The crystal structures of CYP enzymes were retrieved from the protein data bank: CYP1A1 (PDB ID: 4I8V)[51], CYP1B1 (PDB ID:3PMO)[67], CYP1A2 (PDB ID:2HI4)[52], CYP3A4 (PDB ID: 4NY4)[68] and CYP2D6 (PDB ID: 4WNT)[69]. The structures were subjected to protein preparation wizard facility under default conditions implemented in Maestro v9.0 and Impact program v5.5 (Schrodinger, Inc., New York, NY, 2009). The prepared protein was further utilized to construct grid file by selecting co-crystallized ligand as centroid of grid box. For standardization of molecular docking procedure co-crystallized ligands such as ANF

(CYP1A1, CYP1B1 and CYP1A2), ajmalicine (CYP2D6) and bromocriptine (CYP3A4) were extracted from prepared enzyme-ligand complexes and re-docked The rest of the chemical structures were sketched, minimized and docked using GLIDE XP. The ligand-protein complexes were minimized using macromodel. In order to determine selectivities, the corresponding binding sites of CYP enzymes 1A1, 1A2, 2D6 and 3A4 were aligned and analysed with respect to CYP1B1.

4.3.17. Statistical Analyses. Data from each experiment was analysed by Microsoft Excel 2010. Using Excel, Student's t tests were performed to compare IC_{50} and EC_{50}values.

ACKNOWLEDGEMENTS. The work was supported by funds from the Edith Murphy Foundation and HEIF-UK (BC). TC gratefully acknowledges support from De Montfort University for a scholarship towards his PhD studies. The EPSRC UK National Mass Spectrometry Facility at Swansea University is also acknowledged for their support.

REFERENCES

[1] F.P. Guengerich, Cytochrome p450 and chemical toxicology, Chem. Res.Toxicol., 21 (2008) 70-83.

[2] F.P. Guengerich, Y.J. Chun, D. Kim, E.M. Gillam, T. Shimada, Cytochrome P450 1B1: a target for inhibition in anticarcinogenesis strategies, Mutat Res., 523-524 (2003) 173-182.

[3] T. Shimada, C.L. Hayes, H. Yamazaki, S. Amin, S.S. Hecht, F.P. Guengerich, T.R. Sutter, Activation of chemically diverse procarcinogens by human cytochrome P-450 1B1, Cancer Res., 56 (1996) 2979-2984.

[4] H. Yamazaki, N. Hatanaka, R. Kizu, K. Hayakawa, N. Shimada, F.P. Guengerich, M. Nakajima, T. Yokoi, Bioactivation of diesel exhaust particle extracts and their major nitrated polycyclic aromatic hydrocarbon components, 1-nitropyrene and dinitropyrenes, by human cytochromes P450 1A1, 1A2, and 1B1, Mutat.Res., 472 (2000) 129-138.

[5] J. Liu, S.F. Taylor, P.S. Dupart, C.L. Arnold, J. Sridhar, Q. Jiang, Y. Wang, E.V. Skripnikova, M. Zhao, M. Foroozesh, Pyranoflavones: a group of small-molecule probes for exploring the active site cavities of cytochrome P450 enzymes 1A1, 1A2, and 1B1, J. Med.Chem., 56 (2013) 4082-4092.

[6] A. Wang, U. Savas, C.D. Stout, E.F. Johnson, Structural characterization of the complex between α-naphthoflavone and human cytochrome CYP1B1, J. Biol. Chem. , 286 (2011) 5736–5743.

[7] J.G. Liehr, M.J. Ricci, 4-Hydroxylation of estrogens as marker of human mammary tumors, Proceedings of the National Academy of Sciences of the United States of America, 93 (1996) 3294-3296.

[8] R.D. Bruno, V.C. Njar, Targeting cytochrome P450 enzymes: a new approach in anti-cancer drug development, Bioorg. Med. Chem., 15 (2007) 5047-5060.

[9] M.C. McFadyen, M.E. Cruickshank, I.D. Miller, H.L. McLeod, W.T. Melvin, N.E. Haites, D. Parkin, G.I. Murray, Cytochrome P450 CYP1B1 over-expression in primary and metastatic ovarian cancer, Br. J. Cancer, 85 (2001) 242-246.

[10] L.H. Patterson, G.I. Murray, Tumour cytochrome P450 and drug activation, Curr. Pharm. Des., 8 (2002) 1335-1347.

[11] J. Cui, S. Li, Inhibitors and prodrugs targeting CYP1: a novel approach in cancer prevention and therapy, Curr. Med. Chem., 21 (2014) 519-552.

[12] V.G. Martinez, R. O'Connor, Y. Liang, M. Clynes, CYP1B1 expression is induced by docetaxel: effect on cell viability and drug resistance, Br. J. Cancer, 98 (2008) 564-570.

[13] D.C. Spink, B.C. Spink, J.Q. Cao, J.A. De Pasqualle, B.T. Pentecost, M.J. Fasco, Y. Li, T.R. Sutter, Differential expression of CYP1A1 and CYP1B1 in human breast epithelial cells and breast tumor cells, Carcinogenesis, 19 (1998) 291-298.

[14] G.I. Murray, M.C. Taylor, M.C. McFadyen, J.A. McKay, W.F. Greenlee, M.D. Burke, W.T. Melvin, Tumor-specific expression of cytochrome P450 CYP1B1. , Cancer Res., 57 (1997) 3026-3031.

[15] C.L. Hayes, D.C. Spink, B.C. Spink, J.Q. Cao, N.J. Walker, T.R. Sutter, 17b-estradiol hydroxylation catalyzed by human cytochrome P450 1B1, Proc. Natl. Acad. Sci. USA, 93 (1996) 9776-9781.

[16] L. Tait, H.D. Soule, J. Russo, Ultrastructural and immunocytochemical characterization of an immortalized human breast epithelial cell line, MCF-10, Cancer Res., 50 (1990) 6087-6094.

[17] M. McFadyen, H. McLeod, F. Jackson, M. W., D. J., M. G., Cytochrome P450 CYP1B1 protein expression: a novel mechanism of anticancer drug resistance, Biochem. Pharmacol., 62 (2001) 207–212.

[18] B. Rochat, J.M. Morsman, G.I. Murray, W.D. Figg, H.L. McLeod, Human CYP1B1 and anticancer agent metabolism: mechanism for tumor-specific drug inactivation? , J. Pharmacol. Exp. Ther., 296 (2001) 537–541.

[19] I. Bieche, I. Girault, E. Urbain, S. Tozlu, R. Lidereau, Relationship between intratumoral expression of genes coding for xenobiotic-metabolizing enzymes and benefit from adjuvant tamoxifen in estrogen receptor alpha-positive postmenopausal breast carcinoma, Breast Cancer Res., 6 (2003) R252-R263.

[20] B.L. Brockdorff, J. Skouv, B.E. Reiter, A.E. Lykkesfeldt, Increased expression of cytochrome p450 1A1 and 1B1 genes in antiestrogen-resistant human breast cancer cell lines., Int. J. Cancer, 88 (2000) 902-906.

[21] P. Fritz, T.E. Murdter, M. Eichelbaum, I. Siegle, M. Weissert, U.M. Zanger, Microsomal epoxide hydrolase expression as a predictor of tamoxifen response in primary breast cancer: a retrospective exploratory study with long-term follow-up, J. Clin. Oncol., 19 (2001) 3-9.

[22] C.K. Osborne, V.J. Wiebe, W.L. McGuire, D.R. Ciocca, M.W. DeGregorio, Tamoxifen and the isomers of 4-hydroxytamoxifen in tamoxifen-resistant tumors from breast cancer patients., J. Clin. Oncol., 10 (1992) 304-310.

[23] F. Li, C. Jiang, M.C. Larsen, J. Bushkofsky, K.W. Krausz, T. Wang, C.R. Jefcoate, F.J. Gonzalez, Lipidomics reveals a link between CYP1B1 and SCD1 in promoting obesity, Journal of proteome research, 13 (2014) 2679-2687.

[24] C.Y. Song, K. Ghafoor, H.U. Ghafoor, N.S. Khan, S. Thirunavukkarasu, B.L. Jennings, A.M. Estes, S. Zaidi, D. Bridges, P. Tso, F.J. Gonzalez, K.U. Malik, Cytochrome P450

1B1 Contributes to the Development of Atherosclerosis and Hypertension in Apolipoprotein E-Deficient Mice, Hypertension, 67 (2016) 206-213.

[25] E.C. Vasquez, V.A. Peotta, A.L. Gava, T.M. Pereira, S.S. Meyrelles, Cardiac and vascular phenotypes in the apolipoprotein E-deficient mouse, J. Biomed. Sci., 19 (2012) 22-29.

[26] Y.J. Chun, C. Lim, S.O. Ohk, J.M. Lee, J.H. Lee, S. Choic, S. Kim, trans-Stilbenoids: potent and selective inhibitors for human cytochrome P450 1B1, Med. Chem. Comm., 2 (2011) 402-405.

[27] R. Mikstacka, M. Wierzchowski, Z. Dutkiewicz, A. Gielara-Korzanska, A. Korzanski, A. Teubert, S. Sobiaka, W. Baer-Dubowska, 3,4,2'-Trimethoxy-trans-stilbene – a potent CYP1B1 inhibitor, Med. Chem. Comm., 5 (2014) 496-501.

[28] H. Takemura, T. Itoh, K. Yamamoto, H. Sakakibara, K. Shimoi, Selective inhibition of methoxyflavonoids on human CYP1B1 activity, Bioorg. Med. Chem., 18 (2010) 6310–6315.

[29] V.P. Androutsopoulos, A. Papakyriakou, D. Vourloumis, D.A. Spandidos, Comparative CYP1A1 and CYP1B1 substrate and inhibitor profile of dietary flavonoids, Bioorg. Med. Chem., 19 (2011) 2842-2849.

[30] J. Cui, S. Li, Structure, chemistry and pharmacology of naphthoflavones, Mini Rev. Med. Chem., 13 (2013) 1357-1368.

[31] J. Cui, Q. Meng, X. Zhang, Q. Cui, W. Zhou, W. Li, Design and synthesis of new α-naphthoflavones as cytochrome P450 (CYP) 1B1 inhibitors to overcome docetaxel-resistance associated with CYP1B1 overexpression, J. Med.Chem., 58 (2015) 3534−3547.

[32] D.K. Mahapatra, S.K. Bharti, V. Asati, Chalcone scaffolds as anti-infective agents: Structural and molecular target perspectives, Eur. J. Med. Chem., 101 (2015) 496-524.

[33] D.K. Mahapatra, S.K. Bharti, V. Asati, Chalcones: Structural and molecular target perspectives, Eur. J. Med. Chem., 98 (2015) 69-114.

[34] S.L. Zaidi, S. Mittal, M.S. Rajala, F. Avecilla, M. Husain, A. Azam, Synthesis, characterization and antiamoebic activity of chalcones bearing N-substituted ethanamine tail, Eur. J. Med. Chem., 98 (2015) 179-189.

[35] D.K. Mahapatra, V. Asati, S.K. Bharti, Chalcones and their therapeutic targets for the management of diabetes: Structural and pharmacological perspectives, Eur. J. Med. Chem., 92 (2015) 839-865.

[36] M. Das, K. Manna, Chalcone scaffold in anticancer armamentarium: A molecular insight, J. Toxicol., (2016) 7651047.

[37] D.K. Mahapatra, S.K. Bharti, Therapeutic potential of chalcones as cardiovascular agents, Life Sci., 148 (2016) 154-172.

[38] B. Mathew, A. Haridas, J. Suresh, G.E. Mathew, G. Uçar, V. Jayaprakash, Monoamine oxidase inhibitory action of chalcones: A mini review, Cent. Nerv. Syst. Agents Med. Chem., 16 (2016) 120-136.

[39] A.J. León-González, N. Acero, D. Muñoz-Mingarro, I. Navarro, C. Martín-Cordero, Chalcones as promising lead compounds on cancer therapy, Curr. Med. Chem., 22 (2015) 3407-3425.

[40] K. Monostory, V. Tamasi, L. Vereczkey, P. Perjesi, A study on CYP1A inhibitory action of E-2-(4'-methoxybenzylidene)-1-benzosuberone and some related chalcones and cyclic chalcone analogues, Toxicology, 184 (2003) 203-210.

[41] C. Gaudineau, K. Auclair, Inhibition of human P450 enzymes by nicotinic acid and nicotinamide, Biochem. Biophys. Res. Commun., 317 (2004) 950-956.

[42] C. Pouget, C. Fagnere, J.P. Basly, A.E. Besson, Y. Champavier, G. Habrioux, A.J. Chulia, Synthesis and aromatase inhibitory activity of flavanones, Pharm. Res., 19 (2002) 286-291.

[43] C. Pouget, C. Fagnere, J.P. Basly, G. Habrioux, A.J. Chulia, New aromatase inhibitors. Synthesis and inhibitory activity of pyridinyl-substituted flavanone derivatives, Bioorg. Med. Chem. Lett., 12 (2002) 1059-1061.

[44] S. Bhagat, R. Sharma, D.M. Sawant, L. Sharma, C.A. K., LiOH•H2O as a novel dual activation catalyst for highly efficient and easy synthesis of 1,3-diaryl-2-propenones by Claisen–Schmidt condensation under mild conditions, J. Mol. Catal., 244 (2006) 20-24.

[45] K. Mogilaiah, R.B. Rao, Claisen-Schmidt condensation in the solid state, Indian. J. Chem. Sect. B, 38 (1999) 869-871.

[46] A.A. Duina, M.E. Miller, J.B. Keeney, Budding yeast for budding geneticists: a primer on the Saccharomyces cerevisiae model system, Genetics, 197 (2014) 33-48.

[47] A. Goffeau, B.G. Barrell, H. Bussey, R.W. Davis, B. Dujon, H. Feldmann, F. Galibert, J.D. Hoheisel, C. Jacq, M. Johnston, E.J. Louis, H.W. Mewes, Y. Murakami, P. Philippsen, H. Tettelin, S.G. Oliver, Life with 6000 genes, Science, 274 (1996) 563-567.

[48] S. Kawai, W. Hashimoto, K. Murata, Transformation of Saccharomyces cerevisiae and other fungi: methods and possible underlying mechanism, Bioeng Bugs, 1 (2010) 395-403.

[49] C.L. Crespi, B.W. Penman, D.T. Steimel, T. Smith, C.S. Yang, T.R. Sutter, Development of a human lymphoblastoid cell line constitutively expressing human CYP1B1 cDNA: substrate specificity with model substrates and promutagens, Mutagenesis, 12 (1997) 83-89.

[50] J. Liu, J. Sridhar, M. Foroozesh, Cytochrome P450 family 1 inhibitors and structure-activity relationships, Molecules, 18 (2013) 14470-14495.

[51] A.A. Walsh, G.D. Szklarz, E.E. Scott, Human cytochrome P450 1A1 structure and utility in understanding drug and xenobiotic metabolism, J. Biol. Chem., 288 (2013) 12932-12943.

[52] S. Sansen, J.K. Yano, R.L. Reynald, G.A. Schoch, K.J. Griffin, C.D. Stout, E.F. Johnson, Adaptations for the Oxidation of Polycyclic Aromatic Hydrocarbons Exhibited by the Structure of Human P450 1A2, J. Biol. Chem., 282 (2007) 14348-14355.

[53] I. Chang, Y. Mitsui, S. Fukuhara, A. Gill, D.K. Wong, S. Yamamura, V. Shahryari, Z.L. Tabatabai, R. Dahiya, D.M. Shin, Y. Tanaka, Loss of miR-200c up-regulates CYP1B1 and confers docetaxel resistance in renal cell carcinoma, Oncotarget, 6 (2015) 7774-7787.

[54] P. Kaur, A.R. Chamberlin, T.L. Poulos, I.F. Sevrioukova, Structure-based inhibitor design for evaluation of a CYP3A4 pharmacophore model, J. Med.Chem., 59 (2016) 4210–4220.

[55] I.F. Sevrioukova, T.L. Poulos, Dissecting cytochrome P450 3A4–ligand interactions using ritonavir analogues, Biochemistry, 52 (2013) 4474–4481.

[56] I.F. Sevrioukova, T.L. Poulos, Ritonavir analogues as a probe for deciphering the cytochrome P450 3A4 inhibitory mechanism, Curr. Top. Med. Chem., 14 (2014) 1348–1355.

[57] I.F. Sevrioukova, T.L. Poulos, Structure and mechanism of the complex between cytochrome P4503A4 and ritonavir, Proc. Natl. Acad. Sci. USA, 107 (2010) 18422–18427.

[58] C.E. Gutteridge, J.V. Vo, C.B. Tillett, J.A. Vigilante, J.R. Dettmer, S.L. Patterson, K.A. Werbovetz, J. Capers, D.A. Nichols, A.K. Bhattacharjee, L. Gerena, Antileishmanial and antimalarial chalcones: synthesis, efficacy and cytotoxicity of pyridinyl and naphthalenyl analogs, Med. Chem., 3 (2007) 115-119.

[59] J.A. Geyer, S.M. Keenan, C.L. Woodard, P.A. Thompson, L. Gerena, D.A. Nichols, C.E. Gutteridge, N.C. Waters, Selective inhibition of Pfmrk, a Plasmodium falciparum CDK, by antimalarial 1,3-diaryl-2-propenones, Bioorg. Med. Chem. Lett., 19 (2009) 1982-1985.

[60] M.V. Jyothi, R.Y. Prasad, P. Venkatesh, M. Sureshreddy, Synthesis and antimicrobial activity of some novel chalcones of 3-acetyl pyridine and their pyrimidine derivatives, ChemSci. Trans., 1 (2012) 716-722.

[61] R.D. Gietz, Yeast transformation by the LiAc/SS carrier DNA/PEG method, Methods Mol Biol, 1205 (2014) 1-12.

[62] D. Pompon, B. Louerat, A. Bronine, P. Urban, Yeast expression of animal and plant P450s in optimized redox environments, Methods Enzymol., 272 (1996) 51-64.

[63] F.P. Guengerich, M.V. Martin, C.D. Sohl, Q. Cheng, Measurement of cytochrome P450 and NADPH-cytochrome P450 reductase, Nat. Protoc., 4 (2009) 1245-1251.

[64] E. Paradise, P. Chaturvedi, E. Ter-Ovanesyan, Cytochrome P450 inhibition assays using traditional and fluorescent substrates, Curr. Protoc. Pharmacol., Chapter 7 (2007) Unit 7-11.

[65] S. Mahale, S.B. Bharate, S. Manda, P. Joshi, S.S. Bharate, P.R. Jenkins, R.A. Vishwakarma, B. Chaudhuri, Biphenyl-4-carboxylic acid [2-(1H-indol-3-yl)-ethyl]-methylamide (CA224), a nonplanar analogue of fascaplysin, inhibits Cdk4 and tubulin polymerization: evaluation of in vitro and in vivo anticancer activity, J. Med. Chem., 57 (2014) 9658-9672.

[66] S. Mahale, S.B. Bharate, S. Manda, P. Joshi, P.R. Jenkins, R.A. Vishwakarma, B. Chaudhuri, Antitumour potential of BPT: a dual inhibitor of cdk4 and tubulin polymerization, Cell Death Dis., 6 (2015) e1743.

[67] A. Wang, Uzen Savas, C.D. Stout, E.F. Johnson, Structural Characterization of the Complex between alpha-Naphthoflavone and Human Cytochrome P450 1B1, J. Biol. Chem. , 286 (2011) 5736–5743.

[68] G. Branden, T. Sjogren, V. Schnecke, Y. Xue, Structure-based ligand design to overcome CYP inhibition in drug discovery projects, Drug Discov. Today, 19 (2014) 905-911.

[69] A. Wang, C.D. Stout, Q. Zhang, E.F. Johnson, Contributions of ionic interactions and protein dynamics to cytochrome P450 2D6 (CYP2D6) substrate and inhibitor binding, J. Biol. Chem., 290 (2015) 5092-5104.

FIGURE LEGENDS

Figure 1. (A) Structures of known CYP1 inhibitors **1-5** and structures of newly designed pyridylchalcones **6-7**. (B) Synthesis of pyridyl chalcones **6a-p** and **7a-l**. Reagents and conditions: (i) Method 1. LDA, THF, -78 °C then RT. (ii) Method 2.NaOH (aq), MeOH, 0 °C then RT. (iii) Method 3: solvent-free, RT.

Figure 2. (A). Confirmation of the presence of CYP1B1 protein in adherent HEK293 cells transfected with the plasmid pcDNA3.1/hCYP1B1 via Western blotting. Proteins were fractionated via 10% SDS-polyacrylamide gel electrophoresis (SDS-PAGE) and immunoblotting was performed. 12 µg of protein from HEK293 cells transfected with the plasmid pcDNA3.1/hCYP1B1 (expected size ~60 kDa, Lane 4); 12 µg of protein from HEK293 cells transfected with the empty plasmid pcDNA3.1, containing no insert (Lane 3); 3 µg of protein from CYP1B1-bearing Sacchrosomes (Lane 1); 3 µg of protein from Sacchrosomes isolated from yeast cells that had been transformed with pSYE224 (an empty plasmid, containing no insert; Lane 2). PVDF membrane (Millipore) was used for blotting and the primary and secondary antibodies were from AbCam, Ab 32649 and Ab 6721, respectively. The primary antibody was used at 1:1000 v/v dilution in 1 % dried milk-PBS and polyclonal secondary was used at 1:5000 v/v dilution in 1% dried milk-PBS. (B). EC_{50} values of cisplatin after treatment of cells with a range of concentrations of cisplatin (0.05 µM – 100 µM). The cells used were: (a) untransfected HEK293 cells (HEK293:: –), (b) HEK293 cells transfected with pcDNA3.1 (i.e. HEK293:: pcDNA3.1, the basic plasmid which does not contain a gene insert) and (c) HEK293 cells transfected with pcDNA3.1/hCYP1B1 (i.e. HEK293:: pcDNA3.1/hCYP1B1, the plasmid which encodes the human *CYP1B1* gene). All values, presented in µM concentrations, represent the mean and standard deviations of three independent experiments. (C). EC_{50} values of cisplatin after treatment of HEK293-derived cells with cisplatin and a CYP1B1 inhibitor. A range of concentrations of cisplatin (0.05 µM – 100 µM) were used, in the presence of 2 x IC_{50} values (as was determined in microsomal CYP1B1 assays using Sacchrosomes): [**7k**], 0.02 µM; [**6j**], 0.018 µM; and [ANF], 0.016 µM. The cells used were HEK293 cells transfected with pcDNA3.1/hCYP1B1 (the plasmid which

encodes the human *CYP1B1* gene). All values, presented in µM concentrations, represent the mean and standard deviations of three independent experiments.

Figure 3. (A). CYP1B1 is induced in the ovarian cancer cell line A2780cis, which is resistant to cisplatin, was developed through chronic exposure of the parent cisplatin-sensitive A2780 cell line. 1.74 µg of protein for A2780 and 0.3 µg of protein for A2780cis cells were fractionated by 10% SDS-PAGE followed by immunoblotting. The presence of CYP1B1 protein in A2780cis cells was confirmed by observation of a band with expected size (~60 kDa; Lane 3). CYP1B1 bearing Sacchrosomes acted as positive control (~60 kDa band; Lane 2). Proteins from cells that contained no expression plasmid and A2780 cells acted as controls (Lanes 1 and 4; no CYP1B1 protein was observed). PVDF membrane was used together with polyclonal primary antibody (Ab 32649; 1:1000 v/v dilution in 1% dried milk-PBS) and polyclonal secondary antibody (Ab 6721; 1:5000 v/v dilution in 1% dried milk-PBS) for revelation of the CYP1B1 bands. (B). EC_{50} values of cisplatin after treatment of A2780 derived cells with cisplatin and a CYP1B1 inhibitor. A range of concentrations of cisplatin (0.05 µM – 100 µM) were used, in the presence of 2x IC_{50} values (as has been determined in microsomal CYP1B1 assays using Sacchrosomes): [**7k**], 0.02 µM, [**6j**], 0.018 µM, and [ANF], 0.016 µM. The cells used were HEK293 cells transfected with pcDNA3.1/hCYP1B1 (the plasmid which encodes the human *CYP1B1* gene) and pcDNA3.1 (which does not contain the *CYP1B1* gene). All values, presented in µM concentrations, represent the mean and standard deviations of three independent experiments.

Figure 4. (a) Interactions of ANF (**4**) with CYP1B1. (b) Interactions of **6j** with CYP1B1 (c) Interactions of **7k** with CYP1B1. (d) 3D-Composit map of **6j** with CYP1 family isoforms. (e) The table shows comparison of **6j** and **7k** interactions with CYP1B1, CYP1A2, CYP1A1, CYP2D6 and CYP3A4. NI: no interactions. a indicate flip in orientation of ligand with respect to 6j/7k in CYP1B1 binding cavity.

TABLE LEGENDS

Table 1. Synthetic method, yield and EROD activities of B-ring 3-pyridyl chalcones **6a-p** in Sacchrosomes™

Table 2. Synthetic method, yield and EROD activities of A-ring 3-pyridyl chalcones **7a-l** in Sacchrosomes™

Table 3. Experimental solubility and lipophilicity of ANF (**4**) and pyridyl chalcones **6j** and **7k**

Table 4. The constitution of the regenerating system used per reaction in each single well for different CYPs

Table 5. The constitution of enzyme-substrate mixtures

FIGURES

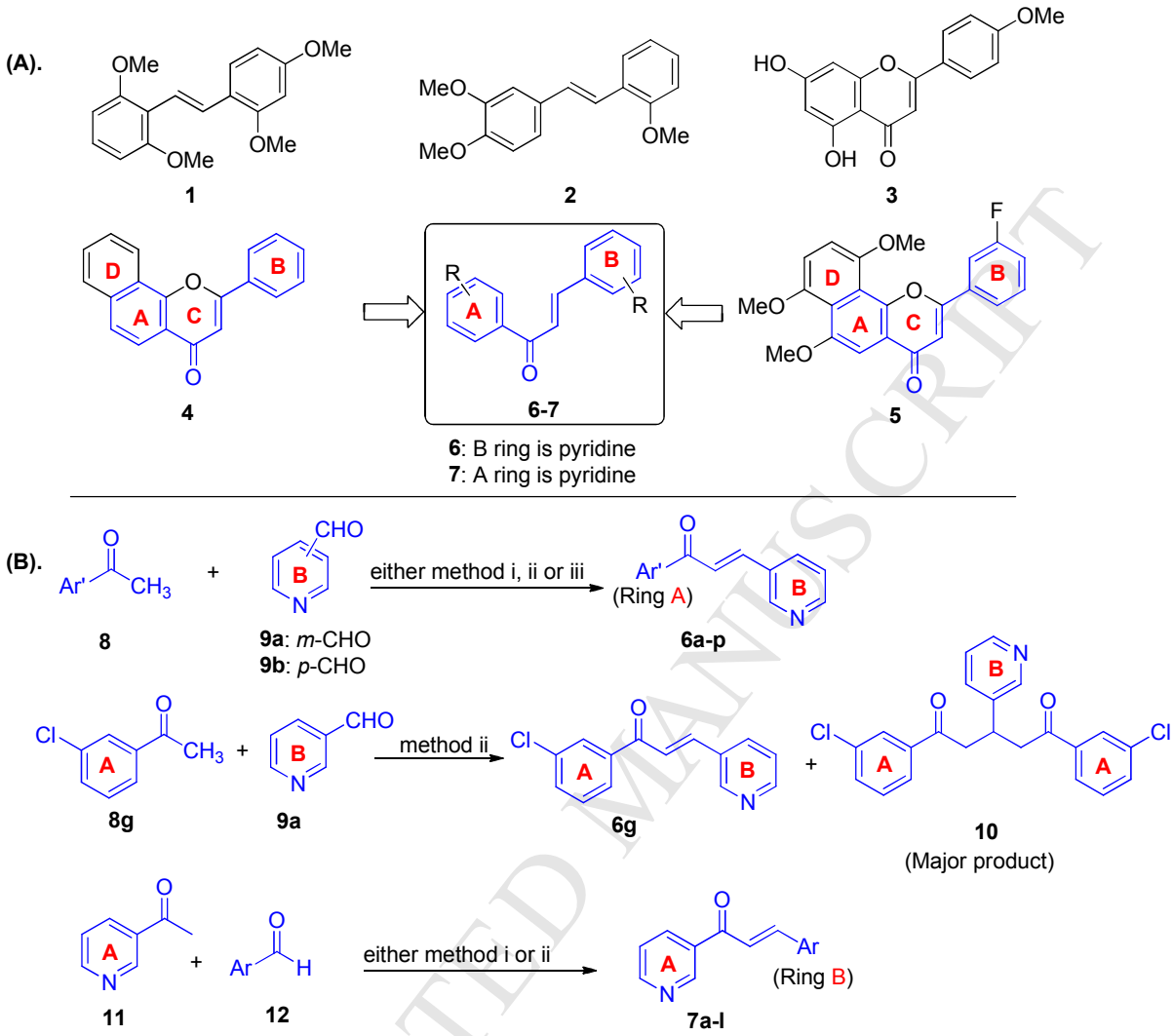

Figure 1. (A) Structures of known CYP1 inhibitors **1-5** and structures of newly designed pyridylchalcones **6-7**. (B) Synthesis of pyridyl chalcones **6a-p** and **7a-l**. Reagents and conditions: (i) Method 1. LDA, THF, -78 °C then RT. (ii) Method 2.NaOH (aq), MeOH, 0 °C then RT. (iii) Method 3: solvent-free, RT.

A.

B.

Cell Line	EC_{50} (µM)
HEK293: –	12 ± 1.1
HEK293: pcDNA3.1	8.7 ± 0.7
HEK293: pcDNA3.1/hCYP1B1	61 ± 8

C.

Cell Line		EC_{50} (µM)		
	Without compound	7k	6j	ANF
HEK293:: pcDNA3.1/hCYP1B1	61 ± 8	1 ± 0.08	8.3 ± 0.6	40 ± 5

Figure 2. (A). Confirmation of the presence of CYP1B1 protein in adherent HEK293 cells transfected with the plasmid pcDNA3.1/hCYP1B1 via Western blotting. Proteins were fractionated via 10% SDS-polyacrylamide gel electrophoresis (SDS-PAGE) and immunoblotting was performed. 12 µg of protein from HEK293 cells transfected with the plasmid pcDNA3.1/hCYP1B1 (expected size ~60 kDa, Lane 4); 12 µg of protein from HEK293 cells transfected with the empty plasmid pcDNA3.1, containing no insert (Lane 3); 3 µg of protein from CYP1B1-bearing Sacchrosomes (Lane 1); 3 µg of protein from Sacchrosomes isolated from yeast cells that had been transformed with pSYE224 (an empty plasmid, containing no insert; Lane 2). PVDF membrane (Millipore) was used for blotting and the primary and secondary antibodies were from AbCam, Ab 32649 and Ab 6721, respectively. The primary antibody was used at 1:1000 v/v dilution in 1 % dried milk-PBS and polyclonal secondary was used at 1:5000 v/v dilution in 1% dried milk-PBS. (B). EC_{50} values of cisplatin after treatment of cells with a range of concentrations of cisplatin (0.05 µM – 100 µM). The cells used were: (a) untransfected HEK293 cells (HEK293:: –), (b) HEK293 cells transfected with pcDNA3.1 (i.e. HEK293:: pcDNA3.1, the basic plasmid

which does not contain a gene insert) and (c) HEK293 cells transfected with pcDNA3.1/hCYP1B1 (i.e. HEK293:: pcDNA3.1/hCYP1B1, the plasmid which encodes the human *CYP1B1* gene). All values, presented in μM concentrations, represent the mean and standard deviations of three independent experiments. (C). EC_{50} values of cisplatin after treatment of HEK293-derived cells with cisplatin and a CYP1B1 inhibitor. A range of concentrations of cisplatin (0.05 μM – 100 μM) were used, in the presence of 2 x IC_{50} values (as was determined in microsomal CYP1B1 assays using Sacchrosomes): [**7k**], 0.02 μM; [**6j**], 0.018 μM; and [ANF], 0.016 μM. The cells used were HEK293 cells transfected with pcDNA3.1/hCYP1B1 (the plasmid which encodes the human *CYP1B1* gene). All values, presented in μM concentrations, represent the mean and standard deviations of three independent experiments.

A.

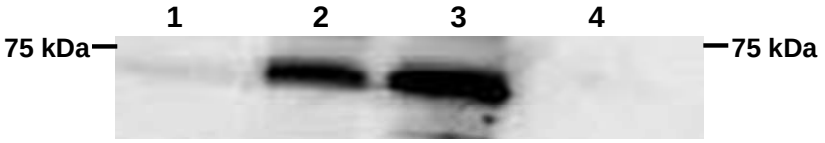

B.

Cell Line	EC_{50} (µM)			
	No Compound	**7k**	**6j**	**ANF**
A2780:: pcDNA3.1/–	3 µM± 0.28	–	–	–
A2780:: pcDNA3.1/hCYP1B1	40 µM± 4.9	0.5± 0.08	3.3 µM± 0.22	35 µM± 4.8

Figure 3. (A). CYP1B1 is induced in the ovarian cancer cell line A2780cis, which is resistant to cisplatin, was developed through chronic exposure of the parent cisplatin-sensitive A2780 cell line. 1.74 µg of protein for A2780 and 0.3 µg of protein for A2780cis cells were fractionated by 10% SDS-PAGE followed by immunoblotting. The presence of CYP1B1 protein in A2780cis cells was confirmed by observation of a band with expected size (~60 kDa; Lane 3). CYP1B1 bearing Sacchrosomes acted as positive control (~60 kDa band; Lane 2). Proteins from cells that contained no expression plasmid and A2780 cells acted as controls (Lanes 1 and 4; no CYP1B1 protein was observed). PVDF membrane was used together with polyclonal primary antibody (Ab 32649; 1:1000 v/v dilution in 1% dried milk-PBS) and polyclonal secondary antibody (Ab 6721; 1:5000 v/v dilution in 1% dried milk-PBS) for revelation of the CYP1B1 bands. (B). EC_{50} values of cisplatin after treatment of A2780 derived cells with cisplatin and a CYP1B1 inhibitor. A range of concentrations of cisplatin (0.05 µM – 100 µM) were used, in the presence of 2x IC_{50} values (as has been determined in microsomal CYP1B1 assays using Sacchrosomes): [**7k**], 0.02 µM, [**6j**], 0.018 µM, and [ANF], 0.016 µM. The cells used were HEK293 cells transfected with pcDNA3.1/hCYP1B1 (the plasmid which encodes the human *CYP1B1* gene) and pcDNA3.1 (which does not contain the *CYP1B1* gene). All values, presented in µM concentrations, represent the mean and standard deviations of three independent experiments.

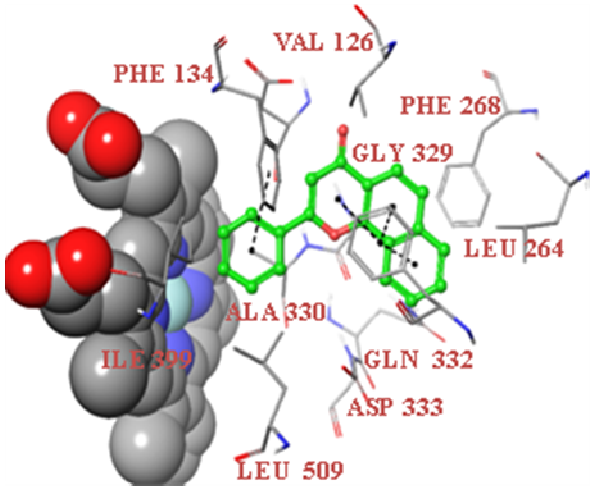

(a)

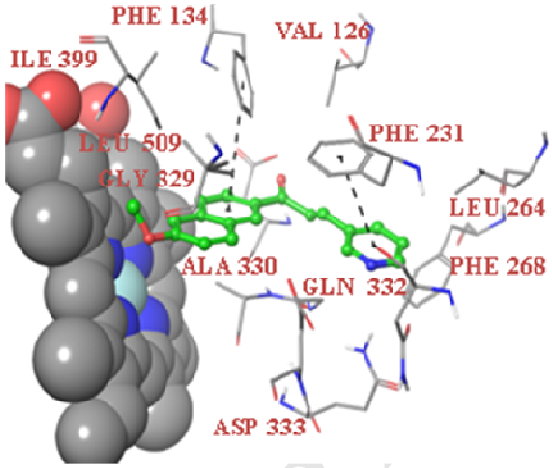

(b)

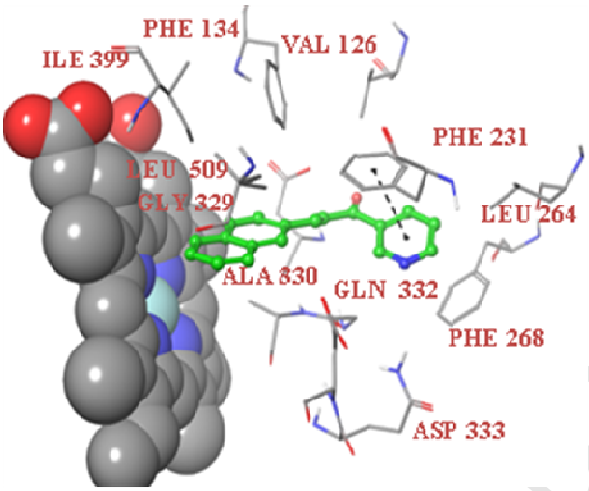

(c)

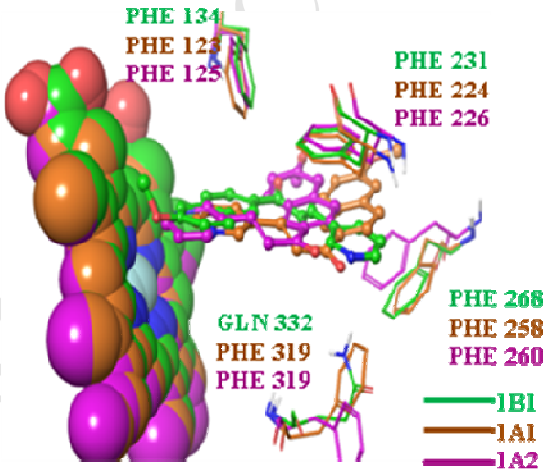

(d)

(e)

CYP	Distance (°A) between **6j** and heme	π-π interactions Ring A	Ring B	Distance (°A) between **7k** and heme	π-π interactions Ring A	Ring B
1B1	4.28	Phe134	Phe231	4.56	Phe231	NI
1A2	4.27 [a]	Phe226	NI	4.18	Phe260	NI
1A1	5.12 [a]	Phe224	NI	4.79 [a]	NI	Phe224
2D6	5.88	Phe483 Phe120	NI	6.43	NI	Phe483 Phe120
3A4	7.5 [a]	Phe215	Phe304	8.06	NI	Phe304

Figure 4. (a) Interactions of ANF (**4**) with CYP1B1. (b) Interactions of **6j** with CYP1B1 (c) Interactions of **7k** with CYP1B1. (d) 3D-Composit map of **6j** with CYP1 family isoforms. (e) The table shows comparison of **6j** and **7k** interactions with CYP1B1, CYP1A2, CYP1A1, CYP2D6 and CYP3A4. NI: no interactions. a indicate flip in orientation of ligand with respect to 6j/7k in CYP1B1 binding cavity.

TABLES

Table 1. Synthetic method, yield and EROD activities of B-ring 3-pyridyl chalcones **6a-p** in Sacchrosomes™

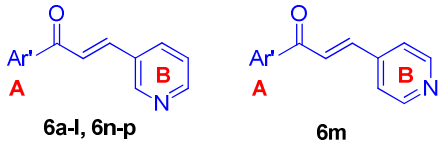

Entry	Ar' (A-ring)	Method	%Yield	Sacchrosome™-bound Enzyme/ IC_{50} µM[a]				
				CYP1B1	CYP1A1	CYP1A2	CYP3A4	CYP2D6
6a	-Ph (3-OMe)	1	25	0.13 ± 0.02	3.5 ± 0.58	0.48 ± 0.08	-	-
6b	-Ph (4-OMe)	1	48	0.525 ± 0.088	3.6 ± 0.60	2.4 ± 0.4	-	-
6c	-Ph (2,4-di-OMe)	1	55	0.093 ± 0.016	1.5 ± 0.25	0.432 ± 0.072	11 ± 1.7	7.7 ± 1.3
6d	-Ph (3,4-di-OMe)	1	37	0.176 ± 0.029	3.1 ± 0.52	0.705± 0.118	-	-
6e	-Ph (3,5-di-OMe)	1	34	0.106 ± 0.018	0.879 ± 0.15	0.306 ± 0.051	-	-
6f	-Ph (2,3,4-tri-OMe)	1	51	0.137 ± 0.023	5.3 ± 0.88	0.176 ± 0.029	-	-
6g	-Ph (3-Cl)	3	52	0.059 ± 0.009	3.4 ± 0.58	0.238 ± 0.039	12.5 ± 2.1	10.6 ± 1.6
6h	-Ph (3-Br)	3	39	0.064 ± 0.011	2.6 ± 0.43	0.162 ± 0.027	14 ± 2.3	8 ± 1.2
6i	-naphth-2-yl	1	52	0.015 ± 0.003	0.349 ± 0.058	0.636 ± 0.106	28± 4.5	4.4± 0.9
6j	-naphth-2-yl (6-OMe)	2	8	0.009± 0.001	0.795± 0.133	1.2 ± 0.2	10.6± 1.8	5.0 ± 1.0
6k	-naphth-1-yl	1	88	0.023 ± 0.004	0.958 ± 0.160	0.214 ± 0.036	6.0 ± 1.2	1.3 ± 0.3
6l	-Ph (4-Ph)	2	27	0.189 ± 0.032	17± 2.8	2.3 ± 0.38	-	-
6m	-naphth-2-yl	3	39	0.187 ± 0.031	0.907± 0.151	0.3 ± 0.05	-	-
6n	-phenanthren-3-yl	2	61	0.048 ± 0.008	0.122± 0.020	1 ± 0.16	26 ± 4.2	12 ± 2.1
6o	-phenylanthren-9-yl	2	61	0.133 ± 0.022	0.058 ± 0.010	0.669 ± 0.110	-	-
6p	-pyren-1-yl	2	54	0.162 ± 0.027	2.2 ± 0.370	2.1± 0.34	-	-
ANF	-	-	-	0.05 ± 0.01	0.01 ± 0.002	0.03 ± 0.01	-	-

[a]The IC_{50} values represent mean and standard deviations (± SD) from three independent experiments. IC_{50} values of compounds **6c**, **6g**, **6h**, **6i**, **6j**, **6k**, **6n** in Sacchrosome-bound CYP2C9 and CYP2C19 are >20 µM.

Table 2. Synthetic method, yield and EROD activities of A-ring 3-pyridyl chalcones **7a-l** in Sacchrosomes™

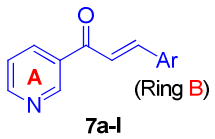

7a-l

Entry	Ar (B-ring)	Method	Yield	Sacchrosome-bound Enzymes/ IC_{50} µM				
			%	CYP1B1	CYP1A1	CYP1A2	CYP3A4	CYP2D6
7a	-Ph (3-OH)	3	17	0.466± 0.078	25.0 ± 4.2	2.9 ± 0.48	-	-
7b	-Ph (3,4-OCH_2O)	2	76	0.029± 0.048	1.5 ± 0.25	1.5 ± 0.25	12 ± 2.1	14 ± 2.2
7c	-Ph (3-OMe)	2	33	0.032± 0.005	10.5 ± 1.8	0.752 ± 0.13	1.28 ± 0.21	1.0 ± 0.16
7d	-Ph (2-OMe)	2	50	0.015± 0.003	4.7 ± 0.8	0.22 ± 0.04	1.52 ± 0.22	1.74 ± 0.30
7e	-Ph (4-OMe, 3-OH)	3	13	0.112± 0.019	2.6 ± 0.4	1.7 ± 0.28	-	-
7f	-Ph (3,4-di-OMe)	3	15	0.019± 0.003	1.4 ± 0.2	0.258 ± 0.04	53.0 ± 8.8	1.1 ± 0.18
7g	-Ph (3,4,5-tri-OMe)	2	37	0.349± 0.058	0.288 ± 0.05	0.515 ± 0.09	-	-
7h	-Ph (2,3,4-tri-OMe)	2	57	0.031± 0.005	0.297 ± 0.05	0.168 ± 0.03	11.8 ± 1.9	8.8 ± 1.5
7i	-Ph (3,4-di-Cl)	2	70	0.096± 0.019	2.0 ± 0.33	0.624 ± 0.11	15 ± 2.5	10.2 ± 1.6
7j	-Ph (3,4-di-F)	2	13	0.12± 0.02	11.8 ± 0.02	0.86 ± 0.14	-	-
7k	-naphth-2-yl	3	29	0.010± 0.001	0.742 ± 1.97	1.2 ± 0.2	18.0 ± 3.1	10.0 ± 1.7
7l	-Ph	2	29	0.077± 0.013	31.8 ± 5.3	4.7 ± 0.78	11.1 ± 1.8	8.2 ± 1.3
ANF	-	-	-	0.05 ± 0.01	0.01 ± 0.002	0.03 ± 0.01	-	-

[a]The IC_{50} values represent mean and standard deviations (± SD) from three independent experiments. IC_{50} values of **7b**, **7c**, **7d**, **7f**, **7h**, **7i**, **7k**, **7l** in Sacchrosome-bound CYP2C9 and CYP2C19 are >20 µM.

Table 3. Experimental solubility and lipophilicity of ANF (**4**) and pyridyl chalcones **6j** and **7k**

	Solubility (Mean ± SD) in µg/mL			**Lipophilicity (Mean ± SD)**	
	PBS	SGF	SIF	Log P	Log D
Entry	(pH 7.4)	(pH 1.2)	(pH 6.8)	(partition coefficient- water/*n*-octanol)	(distribution coefficient- PBS pH 7.4 / *n*-octanol)
ANF (4)	6.85 ± 3.58	6.45 ± 0.28	0.58 ± 0.22	4.52 ± 0.15	4.87 ± 0.31
6j	20.07 ± 0.03	538.43 ± 13.18	0.27 ± 0.28	3.81 ± 0.48	4.42 ± 0.03
7k	14.51 ± 5.94	68.58 ± 12.85	0.45 ± 0.21	4.05 ± 0.14	3.99 ± 0.05

Table 4. The constitution of the regenerating system used per reaction in each single well for different CYPs

Enzyme	Solution A	Solution B	Inhibitor	KPi buffers	water
CYP1A1	5 µl	1 µl	5 µl	39 µl 0.2 M	-
CYP1B1	5 µl	1 µl	5 µl	39 µl 0.2 M	-
CYP1A2	5 µl	1 µl	5 µl	20 µl 0.5 M	19 µl
CYP2D6	5 µl	1 µl	5 µl	25 µl 0.2 M	14 µl
CYP3A4	5 µl	1 µl	5 µl	25 µl 0.2 M	14 µl

Table 5. The constitution of enzyme-substrate mixtures

Enzyme	P450 conc. in Sacchrosomes™	Control Microsome	Substrate	KPi buffers	water
CYP1A1	0.5 µl (0.5 pmole)	2 µl	5 µl 0.1 mM E.R.	425 µl 0.1 M	-
CYP1B1	0.5 µl (0.5 pmole)	1.7 µl	5 µl 0.1 mM E.R.	42.8 µl 0.1 M	-
CYP1A2	1 µl (1 pmole)	1.6 µl	5 µl 320 µM CEC	42.4 µl 0.1 M	-
CYP2D6	2.5 µl (2.5 pmole)	0.4 µl	0.5 µl 2 mM EOMCC	25 µl 0.2 M	21.6 µl
CYP3A4	1.1 µl (1 pmole)	10.102 µl	0.1 µl 2 mM	25 µl 0.2 M	23.96 µl

HIGHLIGHTS

- Potent and highly selective CYP1B1 inhibitors.
- IC_{50} values for CYP1B1 inhibition is 10 and 9 nM.
- Effective in live' yeast and human HEK293 kidney cells.
- Better solubility and lipophilicity values than ANF.
- Overcome cisplatin–resistance in HEK293 and A2780 cells
- Molecular modeling studies performed.